stimulated by the recombinant Ang2. Exposure to 50 μM of MMP inhibitor III, 20 μM of Marimastat (Fig. 5*C*), or 50 μM of GM6001 (data not shown) effectively inhibited the Ang2-stimulated enzymatic activities of MMP-2 in U87MG/Ang2 or the Ang2-stimulated U87MG glioma cells.

Finally, we determined whether Ang2-stimulated *in vitro* cell invasiveness was mediated by modulation of the activation of MMP-2 in glioma cells. We performed the cell invasion assays by using U87MG/Ang2 or parental U87MG cells treated with recombinant Ang2, in the presence or absence of MMP inhibitor III (50 μM) or Marimastat (20 μM). Both MMP inhibitors prevented glioma cell invasion stimulated by Ang2 either by overexpression of Ang2 or by exposure to the recombinant Ang2 (Fig. 5*D*). Thus, Ang2 promotes human glioma cell invasion through the activation of MMP-2 in glioma cells both *in vivo* (Fig. 3) and *in vitro* (Figs. 4 and 5).

Discussion

Although the diverse roles of Ang2 in tumor progression have been studied extensively, investigations of its functions have been primarily focused on its action on angiogenesis through a Tie2-dependent pathway in ECs (6). Increased expression of Ang2 in human tumor tissues or enhanced tumor growth by overexpressing Ang2 in xenografted tumors has been attributed to the effects of Ang2 on ECs (7–11). For example, a recent study that nicely describes a role of Ang2 in gastric cancer progression ascribes the effect of Ang2 on tumor metastases and dissemination to the stimulation of Ang2 on ECs (9). In this report, we present evidence that Ang2 can also directly induce glioma cell invasion in the absence of detectable Tie2 expression. Ectopic expression of Ang2 by U87MG glioma cells conferred an aggressively invasive phenotype to otherwise spheroid-shaped U87MG gliomas. The *in vivo* induction of U87MG glioma invasion by Ang2 was accompanied by increased vessel growth only at the invasive fronts (tumor-adjacent brain parenchyma) of the invading U87MG/Ang2 tumors. Ang2 was also capable of directly inducing invasive behaviors by Tie2-deificent glioma cells *in vitro* where it increased their abilities to invade through Matrigel or VN. These activities were apparent whether the tumor cells expressed the Ang2 or were exposed exogenously to it. Thus, Ang2 is capable of affecting glioma invasion both through its direct activity on Tie2-deficient tumor cells as well as its well documented activity through the Tie2 receptor on EC.

It has been reported that increased expression of MMP-2, MMP-9, and membrane type-1 MMP (MT1-MMP) is correlated with the invasive phenotype of glioma and other types of tumors (2, 17). MT1-MMP is involved in the activation of MMP-2 (17). Although inhibition of MMP-2 expression suppresses the invasiveness of tumor cells in several model systems (14, 18, 19), which molecules induce MMP-2 activation during tumor development has not been defined (17). Our results demonstrate that Ang2 can function as such an inducer and thereby affect glioma cell invasiveness. Interestingly, we also found that MT1-MMP was coexpressed with Ang2 and MMP-2 in the invasive regions in clinical glioma specimens and the Ang2-expressing gliomas (data not shown), suggesting a role for it in Ang2-induced glioma invasion. In contrast, we found diffuse expression of MMP-9 in the invasive Ang2-expressing gliomas, suggesting that it was produced by tumor stroma (20). The responsiveness of the glioma cells to Ang2 even though they lack detectable Tie2 expression raises the question of the details of Ang2 signaling in this case. However, it has been recently reported that Ang2 interacts with certain cell surface integrins to support adhesion for fibroblasts and EC *in vitro* through a Tie2-independent pathway (21). Currently, we are investigating the involvement of integrins and other molecules in modulating the activation of MMP-2 during the Ang2-induced glioma invasion.

In addition to MMPs, compelling evidence shows that integrins (22), urokinase-like plasminogen activator receptor (23), osteopontin, tenasin (24), and SPARC (25) are also involved in glioma invasion. SPARC is an ECM-binding protein that is up-regulated in human primary gliomas. Overexpression of SPARC by U87MG cells induced glioma cell invasion *in vitro* as well as *in vivo* (26). Our studies demonstrate that Ang2 has a similar capacity of inducing glioma cell invasion. Analyses of parental U87MG, LacZ-, or Ang2-expressing cells or various xenografted gliomas derived from these cells showed similar levels of SPARC expression (data not shown). We thus postulate that both SPARC and Ang2 are able to induce glioma invasion with similar phenotypes in brain, and that these two molecules may act independently or synergistically during the glioma progression.

In summary, our data show that in addition to modulating vessel growth, Ang2 is capable of causing MMP-2 activation and thereby inducing glioma cell invasion clearly *in vitro* and may also be of relevance to the *in vivo* setting. We have established a system that should prove useful in deciphering the pathophysiological mechanisms underlying the invasive behaviors of glioma cells *in vivo* and *in vitro*. Defining the pathways by which Ang2 induces tumor invasion could provide critical information with regard to the potential of Ang2 and its effectors as new therapeutic targets in glioma treatment.

We thank M. Jarzynka and F. Cackowski for editing this manuscript; R. Hamilton for the analysis of invasiveness in primary human glioma specimens; S. Rempel, A. W. K Yung, and G. Riggins for advice concerning *in vitro* cell invasion assays; and C. Gladson, W. R. Bishop, C. Counter, and R. Brekken for providing cell lines or reagents. S.-Y.C. is a Sidney Kimmel Scholar and is supported by grants from the Brain Cancer Program of the James S. McDonnell Foundation, the Brain Tumor Society, and the Sidney Kimmel Foundation for Cancer Research, and by developmental funds from the University of Pittsburgh Cancer Institute.

1. Kleihues, P. & Cavenee, W. K. (2000) *Pathology and Genetics of Tumours of the Nervous System* (IARC Press, Lyon, France).
2. Chintala, S. K., Tonn, J. C. & Rao, J. S. (1999) *Int. J. Dev. Neurosci.* 17, 495–502.
3. Brinckerhoff, C. E. & Matrisian, L. M. (2002) *Nat. Rev. Mol. Cell. Biol.* 3, 207–214.
4. Yong, V. W., Power, C., Forsyth, P. & Edwards, D. R. (2001) *Nat. Rev. Neurosci.* 2, 502–511.
5. Lampert, K., Machein, U., Machein, M. R., Conca, W., Peter, H. H. & Volk, B. (1998) *Am. J. Pathol.* 153, 429–437.
6. Yancopoulos, G. D., Davis, S., Gale, N. W., Rudge, J. S., Wiegand, S. J. & Holash, J. (2000) *Nature* 407, 242–248.
7. Ahmad, S. A., Liu, W., Jung, Y. D., Fan, F., Reinmuth, N., Bucana, C. D. & Ellis, L. M. (2001) *Cancer* 92, 1138–1143.
8. Ahmad, S. A., Liu, W., Jung, Y. D., Fan, F., Wilson, M., Reinmuth, N., Shaheen, R. M., Bucana, C. D. & Ellis, L. M. (2001) *Cancer Res.* 61, 1255–1259.
9. Etoh, T., Inoue, H., Tanaka, S., Barnard, G. F., Kitano, S. & Mori, M. (2001) *Cancer Res.* 61, 2145–2153.
10. Koga, K., Todaka, T., Morioka, M., Hamada, J., Kai, Y., Yano, S., Okamura, A., Takakura, N., Suda, T. & Ushio, Y. (2001) *Cancer Res.* 61, 6248–6254.
11. Sfiligoi, C., de Luca, A., Cascone, I., Sorbello, V., Fuso, L., Ponzone, R., Biglia, N., Audero, E., Arisio, R., Bussolino, F., Sismondi, P. & De Bortoli, M. (2003) *Int. J. Cancer* 103, 466–474.
12. Guo, P., Xu, L., Pan, S., Brekken, R. A., Yang, S. T., Whitaker, G. B., Nagane, M., Thorpe, P. E., Rosenbaum, J. S., Su Huang, H. J., *et al.* (2001) *Cancer Res.* 61, 8569–8577.
13. Nakajima, M., Welch, D. R., Wynn, D. M., Tsuruo, T. & Nicolson, G. L. (1993) *Cancer Res.* 53, 5802–5807.
14. Koul, D., Parthasarathy, R., Shen, R., Davies, M. A., Jasser, S. A., Chintala, S. K., Rao, J. S., Sun, Y., Benveniste, E. N., Liu, T. J., *et al.* (2001) *Oncogene* 20, 6669–6678.
15. Lal, A., Glazer, C. A., Martinson, H. M., Friedman, H. S., Archer, G. E., Sampson, J. H. & Riggins, G. J. (2002) *Cancer Res.* 62, 3335–3339.
16. Kheradmand, F., Rishi, K. & Werb, Z. (2002) *J. Cell Sci.* 115, 839–848.
17. Sternlicht, M. D. & Werb, Z. (2001) *Annu. Rev. Cell Dev. Biol.* 17, 463–516.
18. Price, A., Shi, Q., Morris, D., Wilcox, M. E., Brasher, P. M., Rewcastle, N. B., Shalinsky, D., Zou, H., Appelt, K., Johnston, R. N., *et al.* (1999) *Clin. Cancer Res.* 5, 845–854.
19. Fang, J., Shing, Y., Wiederschain, D., Yan, L., Butterfield, C., Jackson, G., Harper, J., Tamvakopoulos, G. & Moses, M. A. (2000) *Proc. Natl. Acad. Sci. USA* 97, 3884–3889.
20. Coussens, L. M., Tinkle, C. L., Hanahan, D. & Werb, Z. (2000) *Cell* 103, 481–490.
21. Carlson, T. R., Feng, Y., Maisonpierre, P. C., Mrksich, M. & Morla, A. O. (2001) *J. Biol. Chem.* 276, 26516–26525.
22. Giannelli, G., Astigiano, S., Antonaci, S., Morini, M., Barbieri, O., Noonan, D. M. & Albini, A. (2002) *Clin. Exp. Metastasis* 19, 217–223.
23. Mohanam, S., Chintala, S. K., Go, Y., Bhattacharya, A., Venkaiah, B., Boyd, D., Gokaslan, Z. L., Sawaya, R. & Rao, J. S. (1997) *Oncogene* 14, 1351–1359.
24. Gladson, C. L. (1999) *J. Neuropathol. Exp. Neurol.* 58, 1029–1040.
25. Rempel, S. A., Golembieski, W. A., Fisher, J. L., Maile, M. & Nakeff, A. (2001) *J. Neurooncol.* 53, 149–160.
26. Schultz, C., Lemke, N., Ge, S., Golembieski, W. A. & Rempel, S. A. (2002) *Cancer Res.* 62, 6270–6277.

悪性脳腫瘍治療の最近のトピックス

ナビゲーション手術・脳機能マッピング・術中蛍光診断・テーラーメイド治療について

悪性脳腫瘍の代表である悪性神経膠腫は依然難治性疾患で，その予後は現在の集学的治療によってもきわめて不良である。近年のテクノロジーや基礎科学の進歩により可能となってきた手術中の脳機能モニタリング・腫瘍同定法と化学療法のアプローチにつき概説する。

永根基雄[1]

脳腫瘍のなかでも髄膜腫や神経鞘腫などで代表される良性脳腫瘍は，手術およびそれに代替される治療により良好な予後が得られているのに対し，神経膠腫を代表とする悪性脳腫瘍はいまだ治癒が得られる率が低く，特にきわめて悪性の膠芽腫に対しては有効な治療手段をもちえていないのが現状である。近年の分子生物学やテクノロジーなどの基礎科学のめざましい発展により新たな診断・治療法の開発が可能となってきており，現在の手術・放射線・化学療法を主体とする治療法への応用がさまざまな形で検討されてきている。

本稿では，そのなかでわれわれの施設でも行っているいくつかのトピックスを紹介する。

術中の腫瘍および神経モニタリング

近年の神経放射線学の技術革新，特にMRIの普及と進歩により，画像による脳腫瘍の描出能力は格段と向上した。それにより手術による腫瘍摘出率や残存腫瘍容量の評価が，以前に増して容易にかつ正確に行うことができるようになり，摘出率と予後の関連性についての再検討が報告されている。

2000年版の日本脳腫瘍統計によれば，手術による腫瘍摘出率と，悪性神経膠腫の予後には相関が認められ[1]，また米国からも同様の報告が出されており[2]，従来の術者の主観的評価を基にした報告ではcontroversialであった摘出率向上の意義が，悪性神経膠腫の予後改善に重要な因子として評価されつつある。

◆腫瘍の局在同定(ナビゲーション手術)

術中に腫瘍の局在を術野で同定するため，脳表からの超音波断層画像は簡便かつreal-timeの脳内腫瘍描出能を有しており，頻用されているが(図1b，2b)，空間解像力が低い点や，手術後半で腫瘍摘出後の切除面に生じるartifactのため，残存腫瘍の評価には難がある。深部あるいは比較的小さい病巣の同定には，image-guideのナビゲーション・システムが有力であり，近年ではMRIとリンクしたStealth Station(メドトロニック・ソファモア・ダネック製)などのシステムが解像度や正確性に優れており，open MRIと連動させた術中MRIは21世紀の手術室には欠かせない設備となっていくものと考えられる(他項を参照)。

われわれは，CT-basedのニューロナビゲーション・システムであるBrain Pointer(三鷹光機製)

1. Nagane M：杏林大学医学部脳神経外科

 0911-1069/03/¥400/論文/JCLS

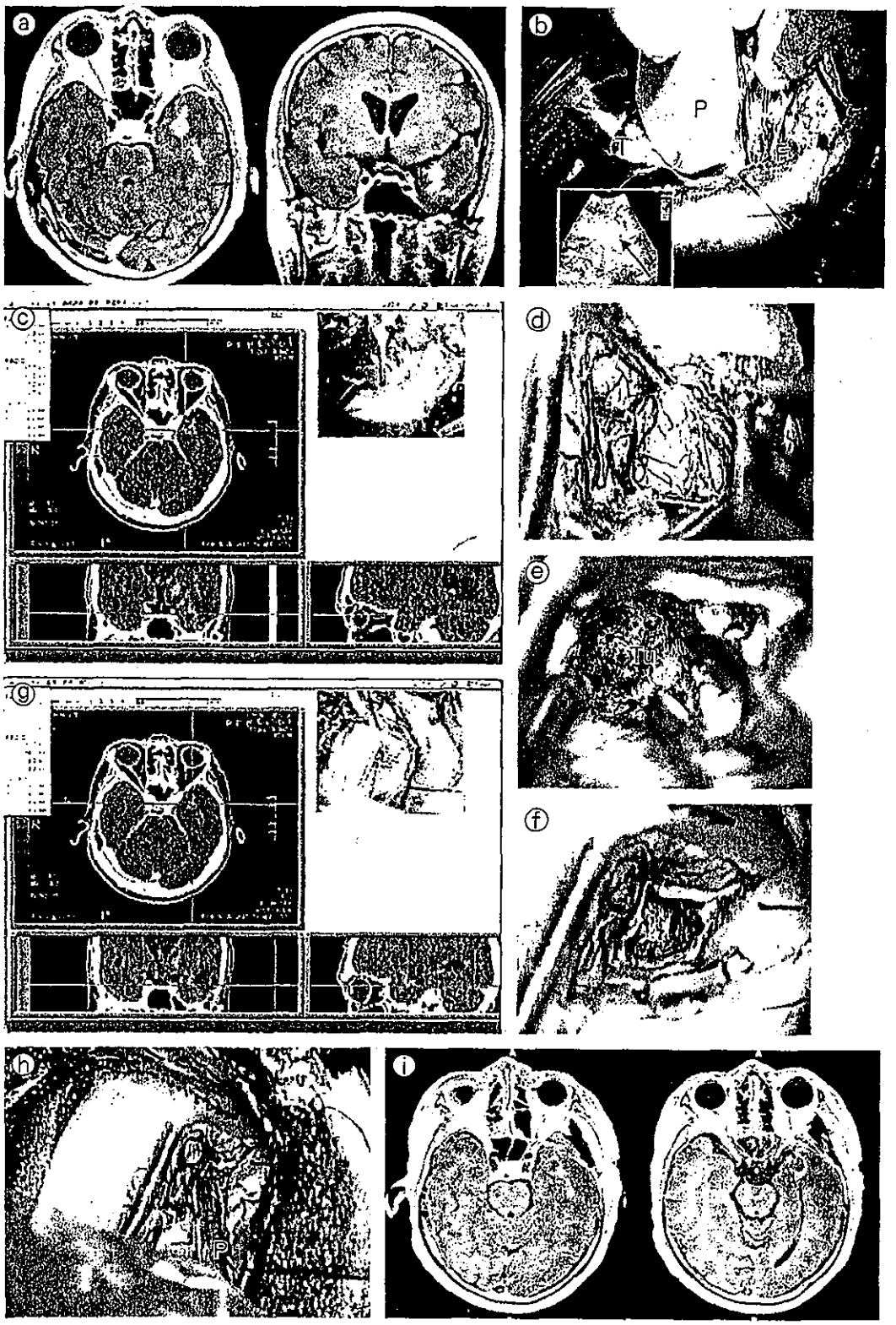

図1　術中ナビゲーション・システム：左側頭葉の悪性リンパ腫症例
a 術前MRI（Gd造影T1強調像）
b 術中超音波像
↑：腫瘍
T：側頭葉
F：前頭葉
P：プローブ
c 術中ナビゲーション画像
プローブ先端が三次元画像上にプロットされる。
d 脳表切開部
e 露出された腫瘍
f 腫瘍摘出後の術中写真
g 腫瘍摘出後のナビゲーション画像
h gのプローブの位置
i 術後MRI
腫瘍のみが摘出されている。

Pitfall

brain shift

・ナビゲーション手術を施行するうえで生じる問題点。通常のナビゲーション手術では，術前に撮像したCTあるいはMRIの画像を基に脳および腫瘍を三次元的に表示し，そのなかに手術中のプローブからの位置情報を投射している。手術中に髄液の排出や脳の圧排・腫瘍除去などの操作により，実際の脳や腫瘍の位置が移動し，モニタ画像上の位置との間にずれが生じてくる。特に腫瘍の摘出が進む手術後半でずれの程度が大きくなるため，使用上注意を要する。この問題を解決するために術中MRIや超音波ガイドによるリアルタイム・ナビゲーション・システムが開発されている。

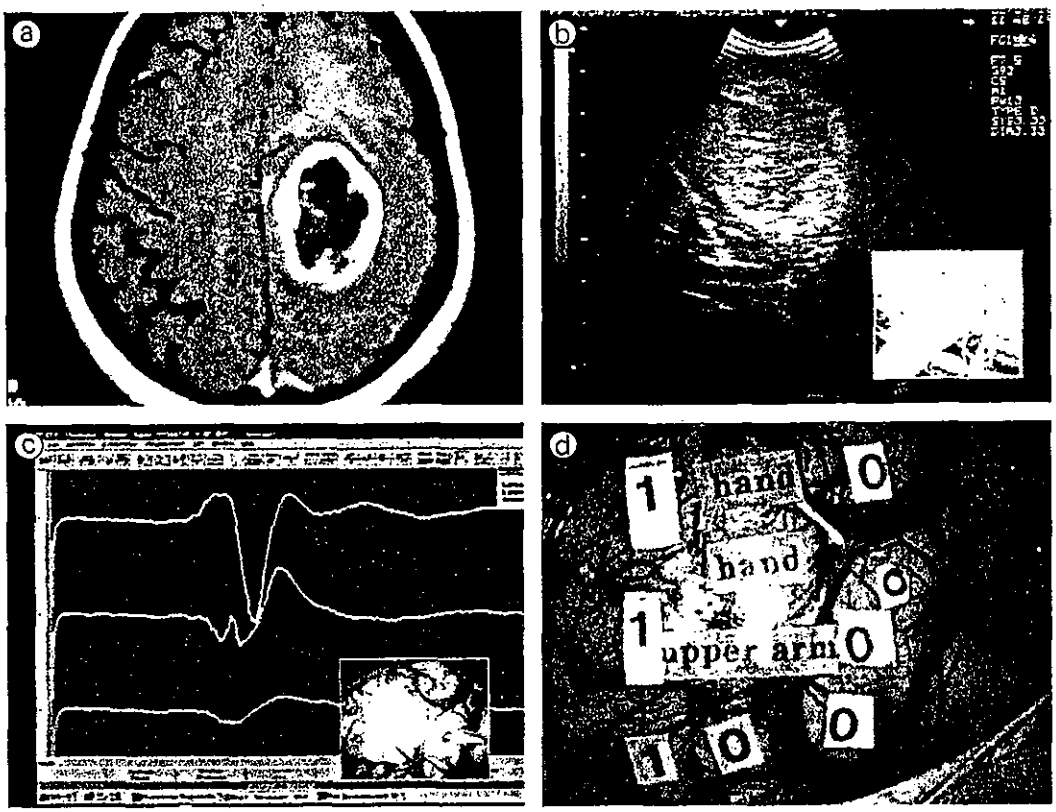

図2　術中脳機能マッピング：左前頭葉膠芽腫
a 術前MRI(Gd造影T1強調像)
b 術中超音波像
c 中心溝同定中のSEPモニタ画像
1番目と2番目の導出の間に波形の逆転が認められ，同部が中心溝と同定された。
d 大脳皮質運動機能マッピング
0：反応なし
1：反応あり

を使用し，正確な術中orientationの確保を試みている。角度計の組み込まれた多関節を有するアームの先端にプローブを設置し，コンピュータ上で仮想先端をプローブの延長上に設定すれば，開頭前に腫瘍の位置をコンピュータの三次元的画像で確認でき，正確で適切な範囲の開頭範囲をデザインする有力な指標となる。開頭後も適宜仮想先端を用いながら脳深部に存在する腫瘍の部位を同定しうるため，安全で最小限の脳皮質切開部位を決定できる。

図1にBrain Pointerの使用が有用であった左側頭葉内の悪性リンパ腫摘出症例を提示する。脳表はまったく正常であり，優位半球でeloquentな皮質を損傷することなく腫瘍の摘出が可能であった。

ナビゲーション手術の難点は，脳変位とよばれる術中の脳実質の移動があげられる。これは硬膜切開後に髄液の流出や，脳の圧排などにより大きく脳の位置がずれることが生じるためで，この問題の解決にはopen MRIや術中脳表超音波プローブなどによる術中の画像更新システムが有望と考えられ，今後，より高精度で簡便なシステムの開発が期待される。

◈脳機能マッピング(神経モニタリング)

実際に腫瘍を摘出する際には，脳表に腫瘍が明らかに露出している以外は，正常脳皮質を切開する必要があり，重要な脳機能の術中損傷を避けるため，大脳皮質表面に電極を設置し，さまざまな脳機能のマッピングを行う必要がある。特に腫瘍が運動領・感覚領・言語領の皮質や皮質直下あるいは近傍に存在する場合(eloquent area)，その局在を術中に把握することが重要となる。脳表からの電気刺激への影響が少ない静脈麻酔薬プロポフォールが導入されて以来，脳神経外科領域の手術において脳機能マッピングを正確に行うことが可能となってきた。

ここでは，プロポフォールを使用した全身麻酔下で施行できる体性感覚誘発電位(somatosensory evoked potential；SEP)と，皮質電気刺激による運動機能マッピングにつき述べる。

◉体性感覚誘発電位(somatosensory evoked potential；SEP)

全身麻酔導入後，通常手関節の正中神経上に針電極を留置する。15mAの刺激により，刺激反対側の頭皮電極から潜時20msecに出現する陰性波

(N20)を導出し，術中持続的SEPモニタリングを行っている。

また，術前のMRI，functional MRI，SAS画像などにより，想定される中心溝を術中に機能的に確認するためにSEPは有用である。脳表を露出後，脳表に中心溝をまたぐように4連電極を矢状方向に設置し，SEP上のN20の位相逆転を検出する。同部位が中心溝と考えられる(図2 c)。

◉運動誘発電位(motor evoked potential；MEP)

腫瘍の局在が運動領あるいは錐体路近傍にある症例では，術中にSEPを用いて中心溝を同定した後，脳表の運動領皮質周辺および腫瘍の直上などを直接電気刺激し，対側の顔面・肩・上下肢に計8カ所の筋電図をモニタすることでMEPを検出し，脳表の運動領マッピングを行っている(図2 c，d，3 b，c)。

電気刺激は単電極を使用して刺激強度を25～35mA，持続時間0.2msec，インターバル1msecの測定条件を用いているが(ニューロパックΣ，日本光電)，電極間が約5mmの双局電極刺激装置を用いている施設も多い。

腫瘍摘出に際して，MEPの検出が良好で腫瘍に近接する脳表皮質上に刺激電極を留置し，数秒間隔の刺激を継続することで，手術操作によるMEP減弱の有無をモニタする。MEPの減弱が生じた場合は手術操作を休止し，回復が認められれば摘出を再開するが，低下が継続する場合は摘出操作を終了する必要がある[3]。

また，腫瘍摘出中に切除面の皮質下電気刺激の併用も試みており，MEPが陽性となった段階が摘出限界と考えられる。

図3　術中運動機能マッピング：右前頭葉膠芽腫

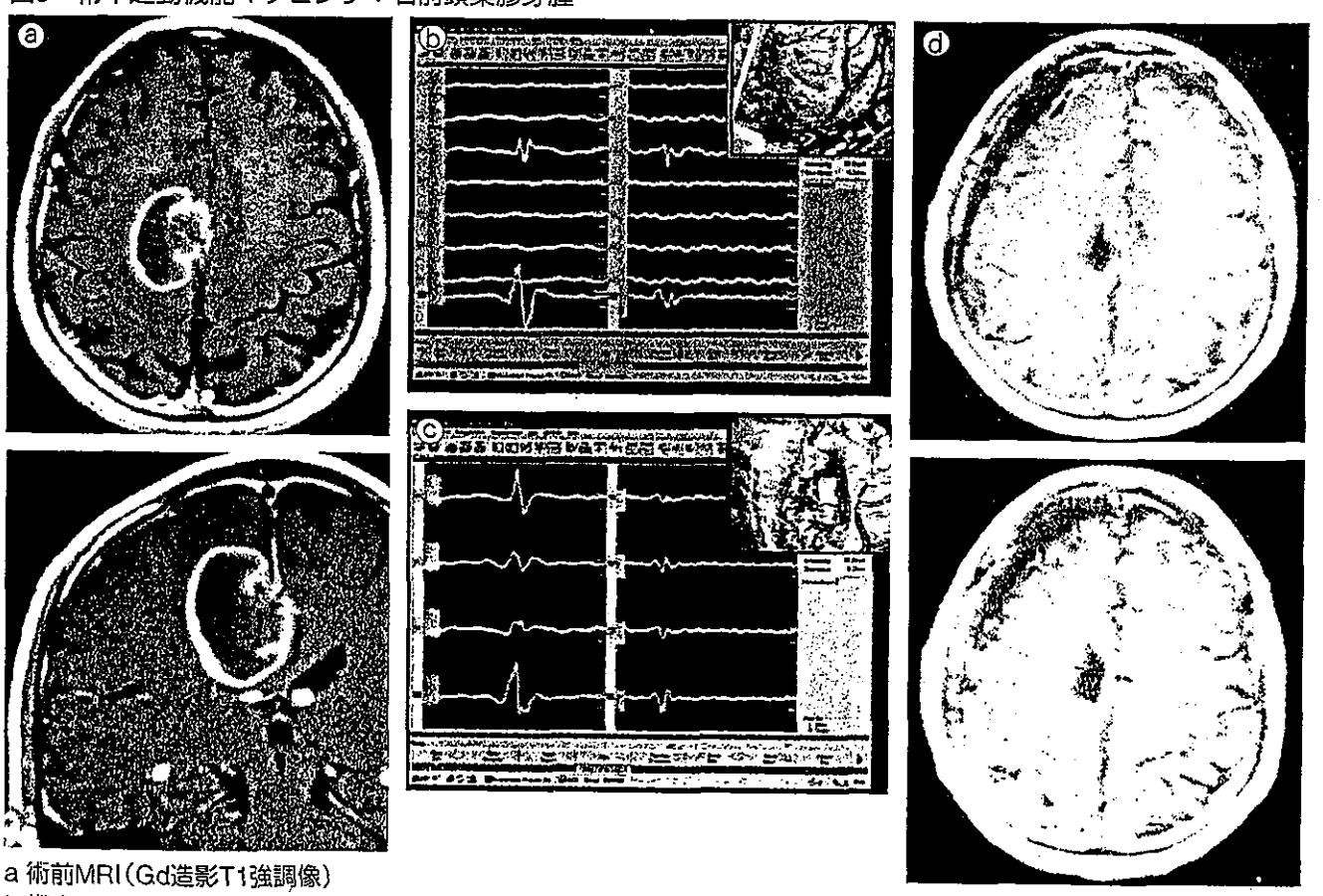

a 術前MRI(Gd造影T1強調像)
b 術中MEPマッピング画面
顔面・肩・上下肢の計8カ所で筋電図を測定。
c 術中持続MEPモニタリング画面
d 術後MRI
腫瘍は全摘されている。
(b，cは稲城市立病院 高遠清太先生より提供)

最近，われわれの施設で術中MEPモニタリングを施行した神経膠腫などのテント上悪性脳腫瘍の20例では，14例(70%)でMEPの術中測定が可能であった。術前の患側四肢麻痺レベル(徒手筋力テスト；MMT)が3/5以上の症例が，そのなかの11例を占め，術前に比較的運動機能が維持されている症例でMEPの検出が良好である傾向が認められた。

一方，術中MEPが検出できなかった6例(30%)では，術前から比較的強度の麻痺(MMT 2/5レベル)が存在した症例が半数を占めた。再発例での運動領皮質の硬膜癒着が強固な場合や，不十分な導出筋電図部位でのモニタなどはMEP検出不良の一因と考えられる。

術中MEPが摘出操作中減弱せず全摘しえた1例では，術後一過性に完全麻痺を呈したものの，約2週間で術前レベルまでの回復が認められ，術中の錐体路障害を示さなかったMEPモニタリングの有用性を示すものと考えられる(図3)。

運動機能に限らず，優位半球の病巣に対しては言語領の同定も重要であり，覚醒下手術を併用しながらの各種脳機能マッピングは不可欠な手術支援技術となってきている。このような神経モニタリングが，eloquent領域にある神経膠腫を主とした悪性脳腫瘍患者の生命，および機能予後の改善にいかに寄与できるかが，今後の検討課題である。

5-aminolevulinic acid (5-ALA) 術中蛍光診断(photodynamic

浸潤性腫瘍である神経膠腫の手術においては，腫瘍を摘出する際に周囲正常脳との境界が不明瞭なため，摘出範囲の決定や残存腫瘍の有無を肉眼的に判断することは一般的に容易ではない。術中に腫瘍を蛍光で発色させるという試みの歴史は古いが，1990年代に入って光源などの技術的問題が改善し，また蛍光物質の開発も進み，近年その有用性が注目されてきている[4]。1997年以降，ドイツを中心に臨床報告がみられる5-ALAを用いた術中蛍光診断は，腫瘍特異性が高いという特性をもち[5]，わが国でも使用する施設が増えてきている[6]。

5-ALAは生体内に存在するヘム生合成の前駆物質であり，それ自体は蛍光物質ではなく，図4に

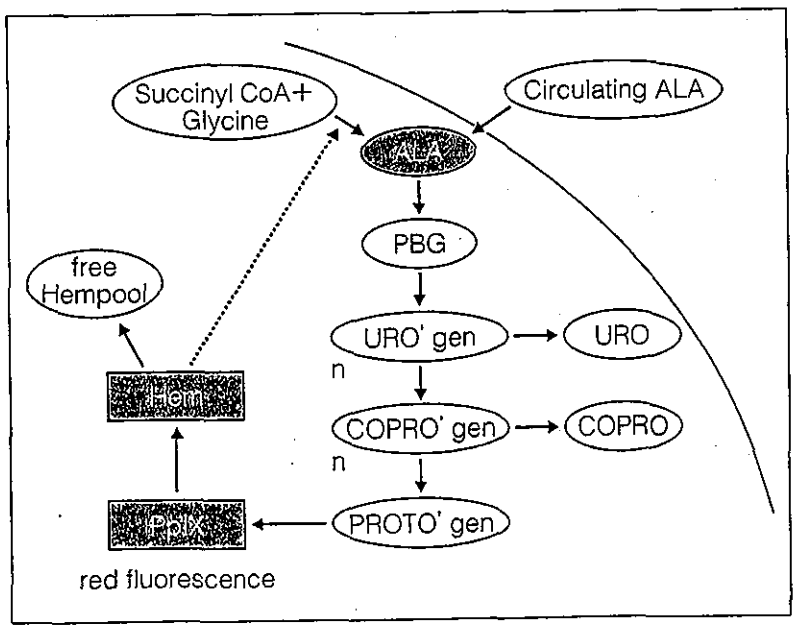

図4　5-ALA代謝経路
経口投与された5-ALAは腫瘍細胞内で蛍光物質であるPpIXに変換される。

用語 a la carte

*1 5-ALA
5-aminolevulinic acid（δ-アミノレブリン酸)の略語。鉄運搬にかかわるヘムの生合成経路の前駆体で生体内に存在する分子。細胞内に移入すると一連の酵素反応によって変換され，赤色の蛍光を発するプロトポルフィリンIX(PpIX)が合成される。5-ALAを過剰に投与することで，ヘムに変換されないPpIXが細胞内に蓄積し，405nmの励起光照射により赤色に発光する。

示すようにいくつかの細胞内酵素反応を介して，細胞内で赤色の蛍光を発するprotoporphyrin (Pp) Ⅸに変換される。5-ALAはそれまでに用いられていたfluorescein sodiumなどの蛍光物質と同様に血液脳関門を通過しないが，腫瘍などの血液脳関門の障害のある病巣に浸透するとともに，代謝の活発な腫瘍細胞内に取り込まれ，代謝蓄積されて蛍光を発するようになる。このPpⅨ生合成に必要な酵素活性は正常脳細胞に比べ悪性腫瘍，特に膠芽腫などで高いことが知られており，腫瘍細胞に特異的な反応とされている。すなわち，理論的には5-ALAが含まれている血液の混入や，脳組織内への浸透だけでは蛍光は誘発されず，低いfalse positivityで，PpⅨが合成された腫瘍細胞を特異的に検出することが可能であろうと考えられる[6]。また，遺伝性ポルフィリン症の患者以外では比較的安全とされている。

5-ALAは経口投与2～6時間後に腫瘍組織内濃度がピークに達し，12時間で消失するため[6]，われわれの施設では手術直前に経口で投与している。術中腫瘍が露出されてから，手術用顕微鏡に搭載されているXenon光源より405nmのフィルターを通して青色の励起光を腫瘍表面に照射し，635nmにピークをもつ赤色のPpⅨ蛍光を455nm～の観察用フィルターを介して肉眼的に観察している(図5，6)。

2002年5月以降に5-ALAによる術中蛍光診断を試みた16例中13例で，明瞭な赤色発光を確認することが可能であった。これら蛍光発光が認められた13症例は，退形成星細胞腫3例，膠芽腫(再発例1例を含む)6例，転移性脳腫瘍4例であり，全例で術前のGd造影MRIにて造影増強効果が認められていた。

一方，悪性リンパ腫はこれまでに脳原発3例，転移性1例で施行したが，いずれも陰性であった。

術中にPpⅨ発光の陽性所見が得られた症例において，肉眼的発光度の程度と腫瘍細胞の密度について病理組織学的に検討すると，術中に強い蛍光強度が得られた部位は，すべて比較的高い細胞密度を示す腫瘍本体の組織像を示していた。一方，腫瘍辺縁で蛍光を認めない部位には明らかな腫瘍細胞を認めなかった。淡い蛍光の部位では，脳組織のなかに腫瘍細胞が巣状にあるいは浸潤しながら存在している症例も認めら

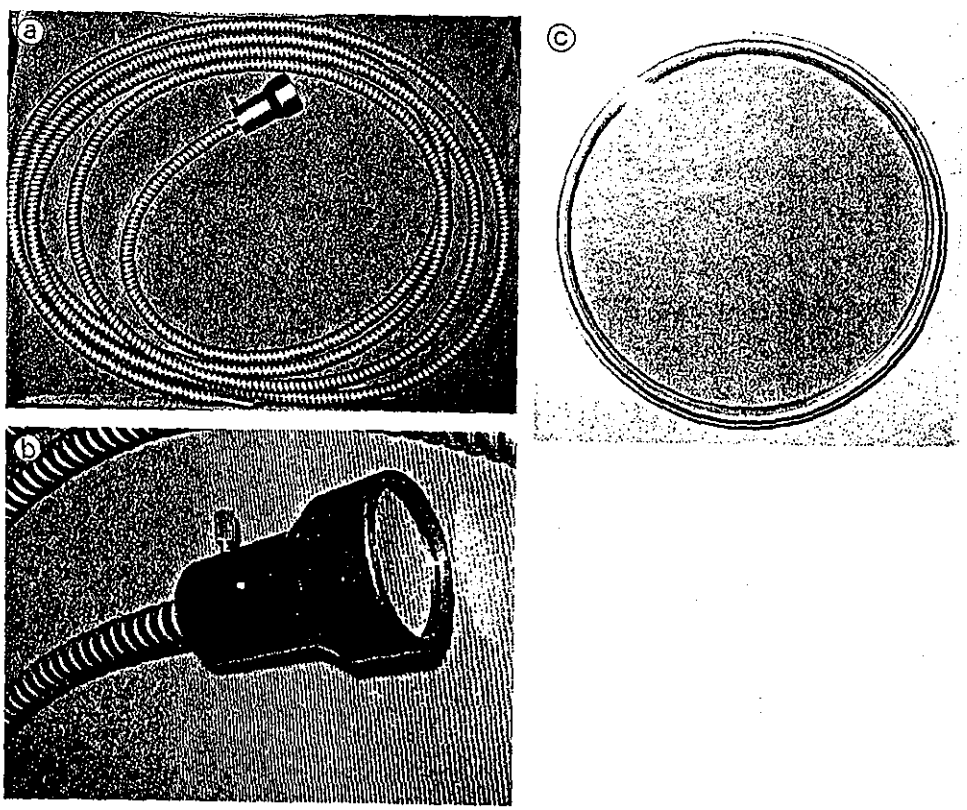

図5　5-ALAによる術中蛍光診断に使用しているファイバーとフィルター
a 手術用顕微鏡のXenon光源から光を誘導するファイバー
b 先端に装着されている405nmフィルター
c PpⅨ発光観察用のlow cutフィルター

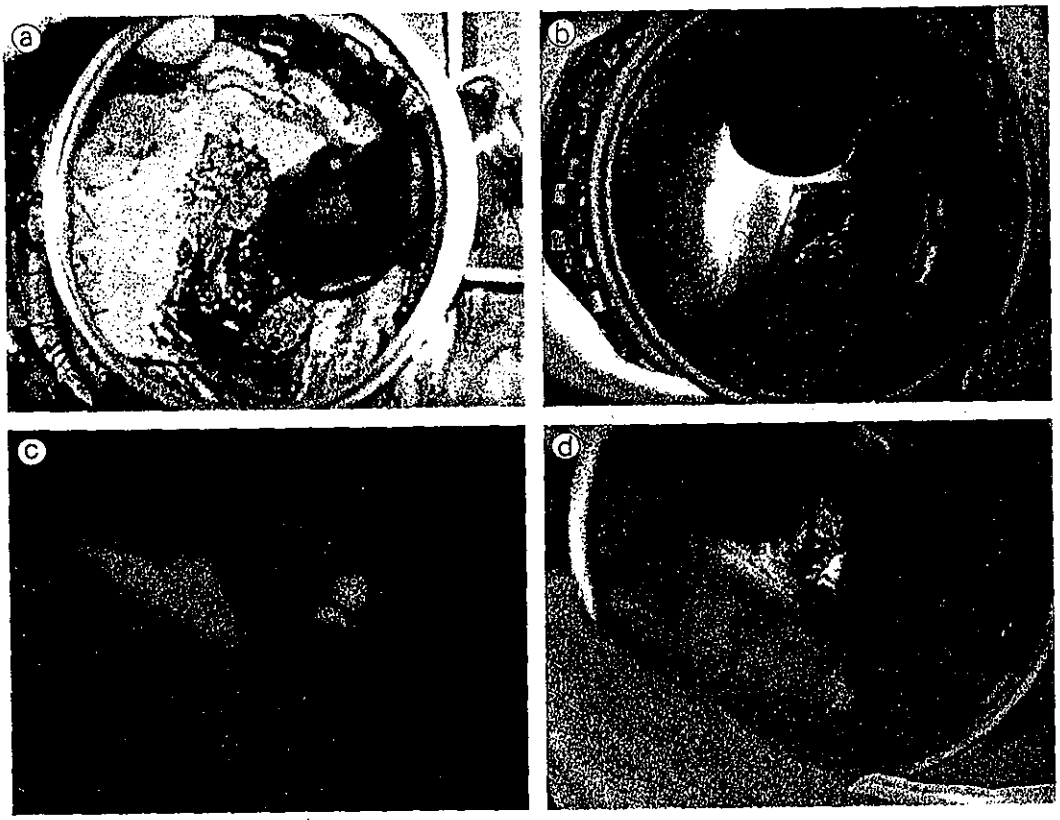

図6　5-ALAによる術中蛍光診断の実際
a 術野にセットされた観察用フィルター
b 青色の励起光を照射すると残存腫瘍が赤色に発光する
c，d PpIX発光陽性の摘出腫瘍片

れ，報告されているようなPpIX蛍光強度と腫瘍細胞密度の相関性は比較的良好なものと考えられる[5]（図7）。したがって，5-ALAによる術中蛍光診断の腫瘍摘出への応用法としては，強度の蛍光を認める部位は積極的に摘出を図ることが望ましく，淡い蛍光が認められる部位には腫瘍以外に正常脳組織も存在している可能性が高く，non-eloquent areaであれば積極的に，eloquent areaであれば慎重にほかのモニタリングなども併用しながら摘出範囲を決定すべきであろう。

今後，MRIで造影効果のみられない低悪性度の神経膠腫などでの検出率の向上や，高感度CCDカメラや強力な励起光光源を備えたbuilt-in microscopeをはじめとしたhardwareの改良が望まれる。5-ALAのみならずNpe6など，ほかの蛍光物質を使用した臨床研究も行われており，また，本法を発展させた形として蛍光発光を利用したphotodynamic therapyによる残存腫瘍の治療も有用性が示されるなど，本アプローチはますます注目されていくことと予想される。

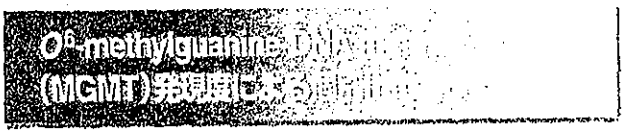

最近，悪性腫瘍に対してもテーラーメイド治療とよばれる個別化治療の必要性が唱えられて

Tips

脳腫瘍の遺伝子異常

・癌化が細胞の遺伝子異常の蓄積により生じることが明らかになってから，脳腫瘍発生に関与する遺伝子異常についても神経膠腫を中心に多数の研究がなされている。星細胞系神経膠腫では癌抑制遺伝子のp53が制御する細胞周期・細胞死の経路（p21，$p14^{ARF}$など）の異常と，網膜芽腫の原因遺伝子であるRbがコアとなる細胞周期制御の経路（癌遺伝子のCyclin D1，CDK4，癌抑制遺伝子のCDKN2A/p16などが関与）の異常が重要であることが明らかになってきた。また最も悪性の膠芽腫では，低悪性度の星細胞腫から悪性転化した"progressive"膠芽腫ではp53の異常が，また先行病変のない"*de novo*"膠芽腫では受容体チロシンキナーゼのEGFRの異常がそれぞれ高頻度で認められ，分子病理学的にはサブタイプの存在が提唱されている。

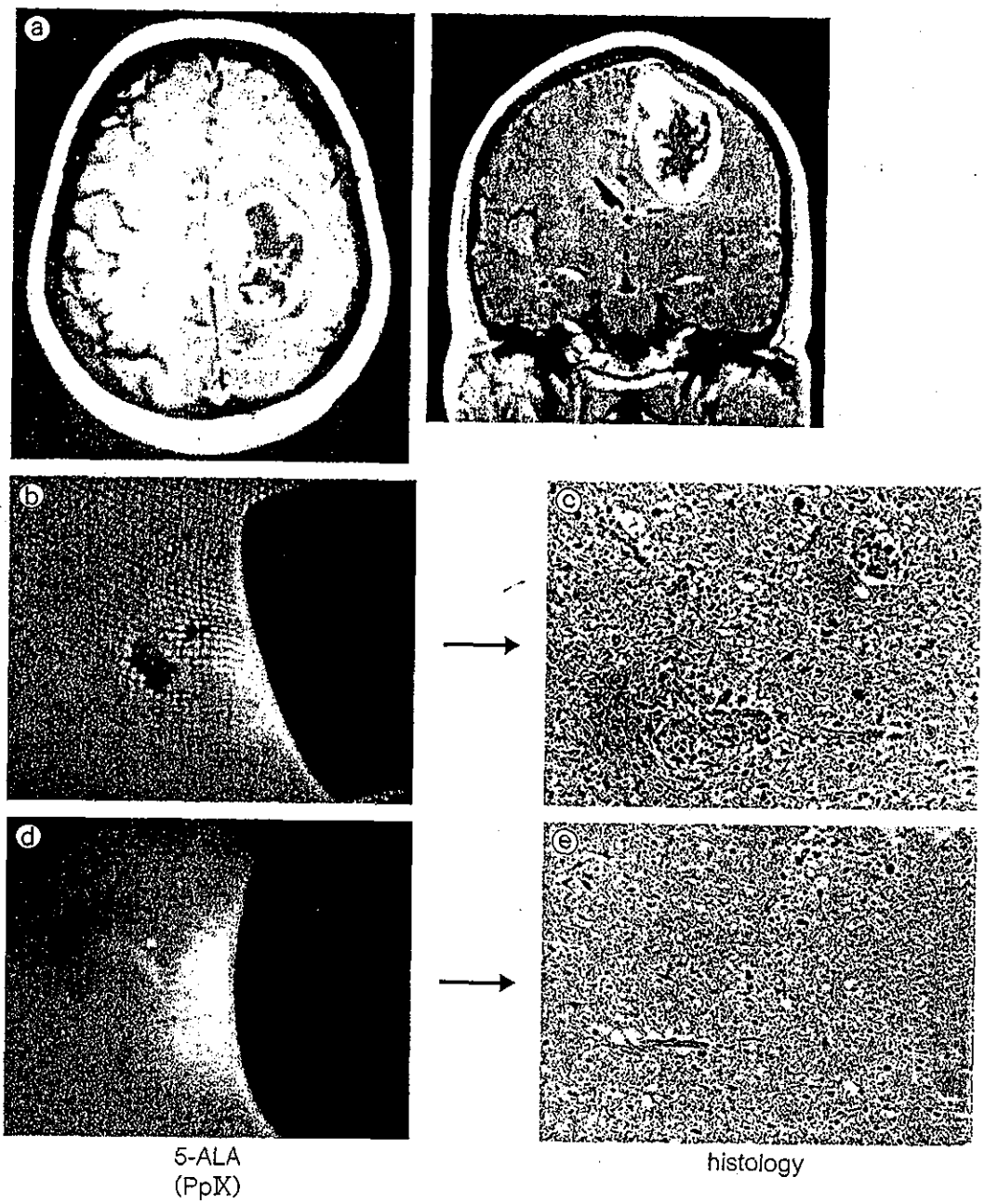

図7　PpIX発光強度と腫瘍細胞密度
a 図2と同一症例。
b，c PpIX発光陽性部分は腫瘍細胞が密に存在した。
d，e 一方，弱陽性部分は正常脳組織のなかに腫瘍細胞の浸潤が認められた。

いる。すなわち個々の患者における治療に際し，行いうる治療法の細かな調節のもとで最も適切な治療を施すことをめざすもので，患者自身と腫瘍自体の両面からのアプローチが存在する。前者については，同じ抗癌剤の治療でもその副作用の程度に個人差があり，そのような「体質」をあらかじめ把握することで，患者別に適切な薬剤と投与量を決定しようとするもので，薬剤代謝酵素の遺伝子などにも多く存在するSNP（単一塩基多型）の研究が大規模に進められている。後者は，直接治療の対象となる腫瘍の薬剤感受性や遺伝子異常の種類を調べることで放射線治療や化学療法への反応性を予見し，より感受性のよい治療プロトコールを選択しようとするものである。

悪性神経膠腫では，術後の放射線治療が延命効果をもつことは明らかにされているが，化学療法の有効性は放射線治療との併用による軽度の延命効果がみられるにとどまっており[7]，いまだ満足のいくものとはいえない。悪性神経膠腫に主に使用されているニトロソウレア剤（chloroethylnitrosourea；CENU）（欧米ではBCNU，わが国ではACNUが主として使用されている）に対し，腫瘍細胞によってはもともと耐性を示す

ものがある。CENUは腫瘍細胞の核DNAのグアニン残基をアルキル化することで殺細胞効果を発揮するが，付加されたアルキル基を特異的にDNAから除去する特殊なDNA修復酵素であるMGMTが発現していると，CENU由来のDNA傷害が正常に修復されてしまい，CENU耐性の原因となると考えられている[8]（図8）。

実際にヒト神経膠腫細胞でMGMT mRNAの発現量と細胞のACNU耐性度との間には良好な相関関係が認められ[9]，約8割の神経膠腫でMGMT活性は陽性である[10]。このような事実から，現在，MGMTの発現量を基にACNUの使用を決定していくテーラーメイド治療が試みられている[11~13]。

われわれの施設でも2000年3月以降，手術摘出腫瘍標本から腫瘍細胞蛋白を抽出し，Western blot法によるMGMT蛋白発現の解析を行っている[14]（図9）。この方法でほとんどの神経膠腫から特異的にMGMT蛋白の発現を確認できた。各腫瘍におけるMGMT蛋白の発現量をβ-actinの発現量で標準化し，ACNU耐性でMGMTを高発現しているT98G細胞でのMGMT発現量を100%として，相対的MGMT蛋白発現量を算定している。

図8　MGMTによるACNU耐性の分子機序

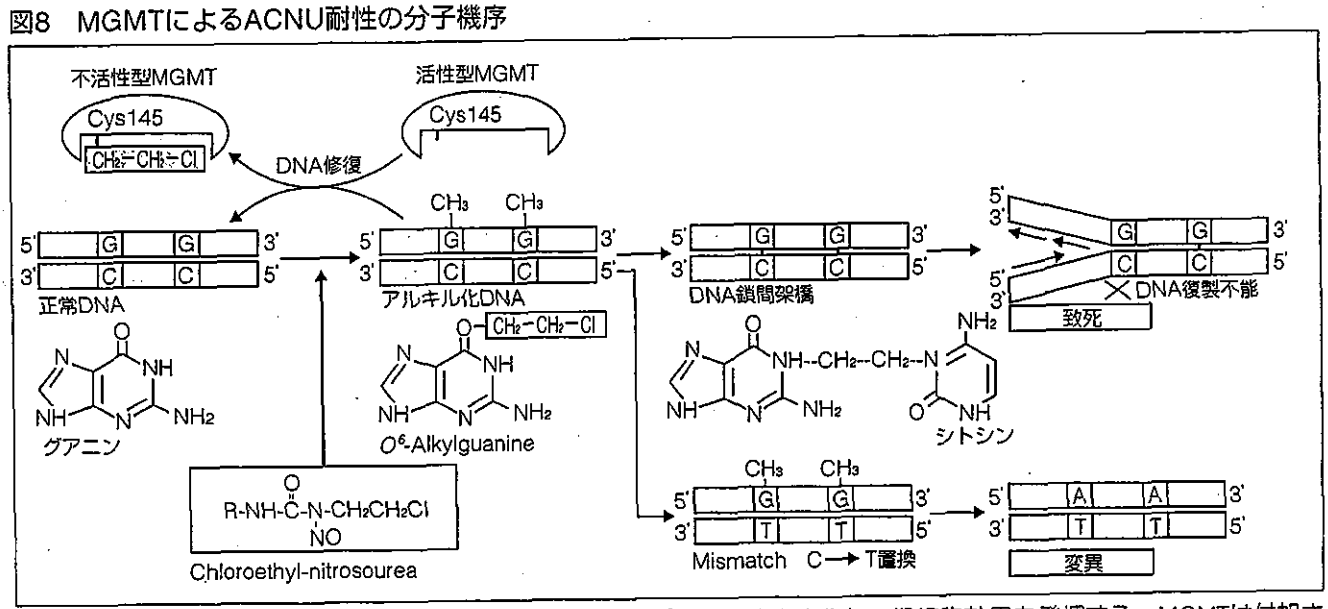

ACNUなどのニトロソウレア剤は，DNAのグアニン残基のO^6位をアルキル化し，殺細胞効果を発揮する。MGMTは付加されたアルキル基を除去することで，DNAを正常化する作用をもつ。
（文献8より引用）

図9　Western blot法によるMGMT蛋白の発現検出

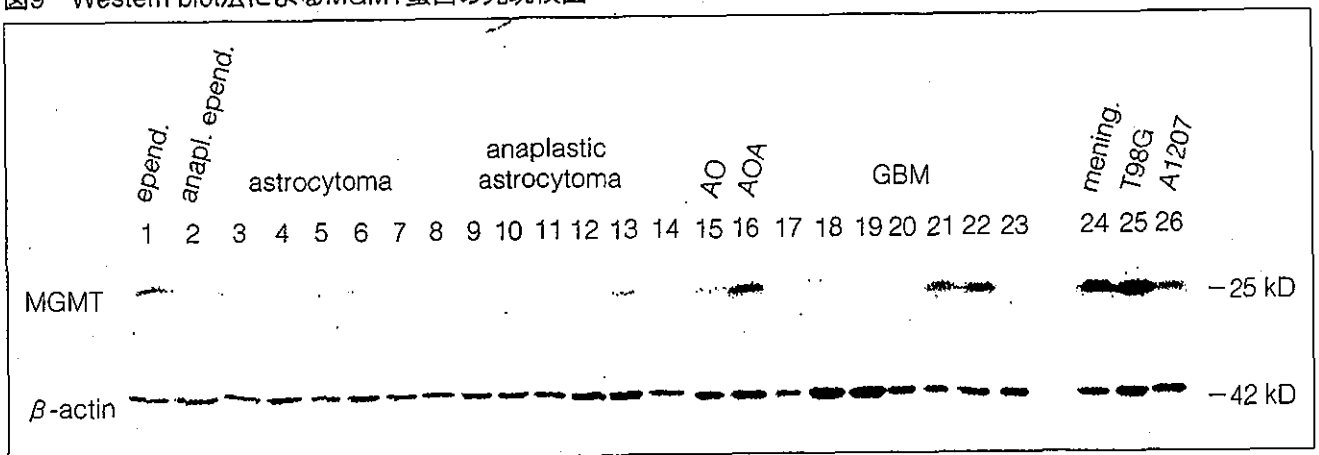

神経膠腫腫瘍標本から抽出した蛋白を電気泳動し，PVDF膜にtransfer後，抗MGMTモノクローナル抗体を用いて約25kDのMGMT蛋白を検出した。β-actinの発現を内部対照として用いた。epend：ependymoma，anapl：anaplastic，AO：anaplastic oligodendroglioma，AOA：anaplastic oligoastrocytoma，GBM：glioblastoma，mening：meningioma
（文献14より一部改変引用）

その結果から悪性神経膠腫に対しては，現在は原則としてMGMTが低発現(T98GのMGMT発現量の20％以下)の腫瘍にはACNUを含む併用化学療法を，高発現(同20％以上)の腫瘍にはACNUを含まない併用化学療法(主としてプラチナ系抗癌剤を使用)を，ともに放射線治療と併用して施行している。

これまで8例の退形成星細胞腫(grade 3)と16例の膠芽腫(grade 4)で検討したが，いずれも半数の症例でMGMTの高発現が認められた。MGMT低発現でACNUを使用した2例の退形成星細胞腫はいまだ再発していないのに対し，MGMT高発現でACNUを使用した2例では(当初はT98GのMGMT発現量に対し30％で選別していたため)，治療開始約半年後に早期の再発をきたした。MGMT低発現でACNUを使用した膠芽腫6例では，半数の3例で1年以上，そのうち2例は1000日以上再発を認めていない。さらにほかの1例は著明な腫瘍縮小がみられた。一方，MGMT高発現でACNU治療を行った3例では，広範な脳葉切除が可能であった1例を除き，いずれも4カ月以内に再発した。ACNU以外を使用した4例でも，全摘しえた1例以外は4カ月以内に再発している[13]。

この結果は，悪性神経膠腫ではMGMT蛋白発現度が生存期間と強い相関を示したとする報告[15]と合致するもので，MGMT低発現の悪性神経膠腫にはACNUを含む術後補助療法が第一選択となろうが，MGMT高発現の腫瘍に対しては代替すべき薬剤・プロトコールは依然確立していないと考えられる。欧米ですでに悪性神経膠腫への有効性が示され，わが国ではまだ未認可であるTemozolomideや，新規の分子標的治療薬の開発が待たれるが，MGMTを一時的に失活させることでACNU耐性克服を図る方法も検討されている。われわれはACNU耐性ラット・グリオーマ細胞株C6ARにおいて，アンチセンスMGMT RNAによるACNU感受性化を報告したが[16]，欧米では強力なMGMT枯渇剤であるO^6-benzylguanineを用いた臨床試験が現在実施されており，今後の成果が期待されている[17]。

薬剤耐性関連遺伝子のほかにも，退形成乏突起膠腫における染色体1番短腕および19番長腕の欠失のように，化学療法感受性と強い相関を示す遺伝子マーカーの存在が明らかにされてきており[18]，腫瘍の遺伝子解析から同じ組織像をとる腫瘍でも異なる治療方針を立てていくテーラーメイド治療が今後推進されていくものと考えられる。

おわりに

悪性神経膠腫治療における最近のトピックスを紹介した。手術をはじめとした本疾患の治療のなかでさまざまな角度から画像診断が重要な役割を果たしていることは明確であり，今後ますますの技術革新と，その臨床応用が難治性脳腫瘍の予後改善に貢献していくことが期待される。

■文献

1) The Committee of Brain Tumor Registry of Japan: Report of Brain Tumor Registry of Japan (1969-1993), 19th ed. Neurol Med chir (Tokyo), 40 (Suppl): 2000.
2) Lacroix M, et al: A multivariate analysis of 416 patients with glioblastoma multiforme; prognosis, extent of resection, and survival. J Neurosurg, 95: 190-198, 2001.
3) 飯野奈央子ほか：運動野近傍の脳腫瘍摘出時の運動誘発電位Motor evoked potential (MEP)によるマッピングとモニタリングの有用性. 医学検査, 51: 1294-1298, 2002.
4) 黒岩敏彦ほか：蛍光色素を用いたグリオーマ手術. 先端医療シリーズ18 脳神経外科 脳腫瘍の最新医療, 高倉公朋編集. 先端医療技術研究所, 東京, 2003, p259-265.
5) Stummer W, et al: Fluorescence-guided resection of

用語 a la carte

＊2 分子標的治療

腫瘍細胞の癌化や増殖に関与する重要な細胞内外の蛋白質・酵素などの分子を，特異的に阻害する薬剤をスクリーニングし，腫瘍細胞の治療に用いる方法である。主として低分子化合物と抗体が開発されている。Bcr-Ablや*erb*B2などのチロシン・キナーゼを主とした癌遺伝子産物や細胞浸潤に関与するマトリックス・プロテアーゼなどを標的とした治療薬がすでに臨床応用されている。

glioblastoma multiforme by using 5-aminolevulinic acid-induced porphyrins ; a prospective study in 52 consecutive patients. J Neurosurg, 93 : 1003-1013, 2000.
6)金子貞男：脳腫瘍に対する光モニタリングーALA induced PpIXによる術中脳腫瘍蛍光診断ー. 脳外, 29 : 1019-1031, 2001.
7)Fine HA, et al : Meta-analysis of radiation therapy with and without adjuvant chemotherapy for malignant gliomas in adults. Cancer, 71 : 2585-2597, 1993.
8)永根基雄ほか：ACNU耐性とMGMTの発現. Mebio, 10 : 107-113, 1993.
9)Nagane M, et al : Expression of O^6-methylguanine-DNA methyltransferase and chloroethylnitrosourea resistance of human brain tumors. Jpn J Clin Oncol, 22 : 143-149, 1992.
10)Silber JR, et al : O^6-methylguanine-DNA methyltransferase activity in adult gliomas ; relation to patient and tumor characteristics. Cancer Res, 58 : 1068-1073, 1998.
11)Nagane M, et al : Investigation of chemoresistance-related genes mRNA expression for selecting anticancer agents in successful adjuvant chemotherapy for a case of recurrent glioblastoma. Surg Neurol, 44 : 462-468 ; discussion 468-470, 1995.
12)Tanaka S, et al : O^6-methylguanine-DNA methyltransferase gene expression in gliomas by means of real-time quantitative RT-PCR and clinical response to nitrosoureas. Int J Cancer, 103 : 67-72, 2003.
13)永根基雄ほか：杏林大学における悪性神経膠腫の治療戦略. Neuro-Oncology, 12 : 2003, in press.
14)永根基雄ほか：薬剤耐性関連遺伝子の蛋白発現量によるグリオーマの個別化化学療法の試み. ポストシークエンス時代における脳腫瘍の研究と治療, 田渕和雄, 白石哲也編集. 九州大学出版, 福岡, 2002, p375-381.
15)Belanich M, et al : Retrospective study of the correlation between the DNA repair protein alkyltransferase and survival of brain tumor patients treated with carmustine. Cancer Res, 56 : 783-788, 1996.
16)Nagane M, et al : Application of antisense ribonucleic acid complementary to O^6-methylguanine-deoxyribonucleic acid methyltransferase messenger ribonucleic acid for therapy of malignant gliomas. Neurosurgery, 41 : 434-440 ; discussion 440-441, 1997.
17)Quinn JA, et al : Phase II trial of carmustine plus O (6)-benzylguanine for patients with nitrosourea-resistant recurrent or progressive malignant glioma. J Clin Oncol. 20 : 2277-2283, 2002.
18)Cairncross JG, et al : Specific genetic predictors of chemotherapeutic response and survival in patients with anaplastic oligodendrogliomas. J Natl Cancer Inst, 90 : 1473-1479, 1998.

グリオーマの化学療法

藤巻 高光（名古屋大学医学部脳神経外科助教授）

脳内に浸潤性に発育する腫瘍であるグリオーマ（glioma：神経膠腫）に対しては、手術摘出のみでは腫瘍の制御はできず、術後の補助療法（adjuvant therapy）が必須である。このうち放射線治療についてはその有効性は証明されてきたが、化学療法については血液脳関門の存在など脳では不利な条件も多く、その効果は確立されたものであるとは言い難かった。しかし化学療法についてもoligodendroglioma（乏突起神経膠腫）でPCV療法（プロカルバジン＋CCNU［lomustine］＋ビンクリスチン 3剤での併用療法）での有効性の報告が相次ぎ[1,2]、さらにこれらの化学療法の有効性が腫瘍の分子生物学的な性質と相関していることが報告[3]されるなど、主としてoligodendroglioma系統ではいくつもの新知見が積み重ねられてきた。Oligodendrogliomaが先行した形になったが、近年astrocytic tumor（星細胞腫、退形成性星細胞腫、膠芽腫）でもいくつかの進展が認められている。本稿ではastrocytic tumorに対する化学療法の2つの話題を紹介する。

Anaplastic astrocytoma、glioblastomaの維持化学療法

Gliomaの維持化学療法の効果については、evidence levelでの証明はなされてこなかった。しかし2002年度まで行われた厚生労働省成人悪性脳腫瘍班研究（班長：野村和弘国立がんセンター中央病院院長）において、gliomaのうちanaplastic astrocytoma（退形成性星細胞腫）とglioblastoma（膠芽腫）について、放射線療法後の維持化学療法の効果がランダム化試験で検討され、効果が実証された。ニムスチン（ACNU：ニドラン®）併用60Gyの局所放射線療法後、化学療法群ではニムスチン80mg/m²を8週間毎に2年間を静注、非投与群では経過観察のみが行われた。この結果、glioblastomaに関しては、腫瘍無再発期間は維持療法無施行群が6カ月、維持療法群が12カ月と、維持療法の有効性を示す結果であった[4]。従来経験的に行われてきた維持化学療法を行ううえで、今後の根拠となるものである。

新経口抗癌剤temozolomide

Temozolomide（TMZ）は新しい経口薬のアルキル化薬である。分子量が194と小さく、血液脳関門を通過する薬剤である（図）。また脂溶性であることは、脂質成分の多い中枢神経系親和性の高い薬剤であるといえる。血清中の濃度の30%が中枢神経系に移行するという。pH 7.0以上のアルカリ性で加水分解され、活性型の5-(3-methyltriazen-1-yl)imidazole-4-carboxamide（MTIC）に変化する、すなわち体内で活性化となる。

欧米では、数年前から種々のgliomaに対して治験が行われた後に、現在ではglioma治療において、特に再発時の標準薬の1つとなりつつある。欧米の治験結果報告によると、最も悪性のgliomaであるglioblastomaの再発に対して、TMZ 150～200mg/m²5日間を4週間周期で投与し、18%の症例で6カ月間再発を認めなかった[5]。また再発anaplastic astrocytoma、anaplastic oligoastrocytomaに対しての多施設共同試験では46%で6カ月間再発がなく、また生存期間の中央値が13.6カ月であったという。画像上の反応でも35%の症例で腫瘍が縮小または消失、25%で腫瘍の増大が停止した[6]。いずれの試験も再発例に対する治療で、かつ単剤の経口薬での治療であることを考えると、注目すべき効果であったといえる。

こういった治験を経てTMZは多くの国ですでにgliomaに対して使用が認められているが、日本ではまだ厚生労働省の認可が得られていない。しかし本年、ようやく日本でもわれわれの施設を含む全国の主要な施設でTMZの治験が開始されようとしている。本薬剤は副作用として血液毒性、また吐き気や嘔吐、便秘などの消化管症状などがあるが、外来経口投与でも治療が可能でありユニークな薬剤である。今回の治験は再発anaplastic astrocytomaに限ったものであるが、本治験が終了し、わが国でもglioma治療に本薬剤が用いられる日が待たれる。

〈参考文献〉
1) Cairncross JG et al：*J Clin Oncol* 8：2090-2091, 1990
2) Mason WP et al：*Neurology* 46：203-207, 1996
3) Cairncross JG et al：*J Natl Cancer Inst* 90：1473-1479, 1998
4) 野村和弘：平成14年度厚生労働省がん研究助成金による研究報告集. p11-19, 国立がんセンター, 2003
5) Brada M et al：*Ann Oncol* 12：259-266, 2001
6) Yung WK：*J Clin Oncol* 17：2762-2771. 1999

図 Temozolomide（分子量194.15）

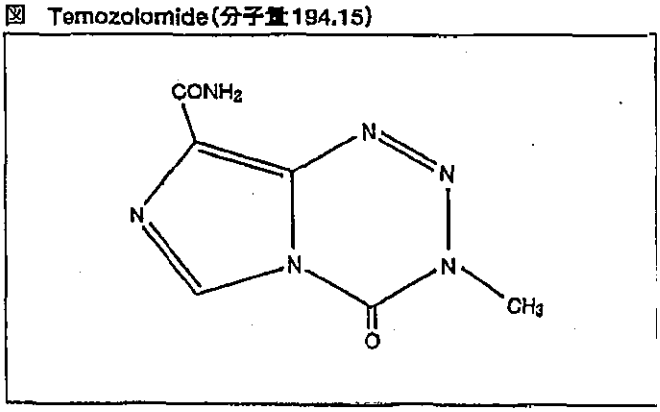

International Congress Series 1256 (2003) 1360

Development of three-dimensional navigation system updated with intraoperative MRI

Y. Muragaki[a,*], K. Suzukawa[b], H. Iseki[a,c], T. Maruyama[c], K. Nambu[a], H. Aramata[a,b], M. Sugiura[a], K. Naemura[a], T. Hori[c], K. Takakura[c]

[a] *Faculty of Advanced Techno-Surgery, Institute of Advanced Biomedical Engineering and Science, Graduate School of Medicine, Tokyo Women's Medical University, Tokyo, Japan*

[b] *Infocom Co., Japan*

[c] *Department of Neurosurgery, Neurological Institute, Tokyo Women's Medical University, Tokyo, Japan*

Received 13 March 2003; received in revised form 13 March 2003; accepted 17 March 2003.

1. Introduction

Navigation system has emerged as a heavyweight in neurosurgery. However, the 2-D images of coventional navigation are not helpful for surgeons to comprehend the place of the region in the surgical field intuitively. To improve the surgeon's intuitive comprehension of spatial localization of their tools, we here report the development of 3-D navigation system updated with intraoperative MRI and its initial experiences of clinical study.

2. Methods

The 3-D navigation system was innovated from a surgical navigation system (PRS navigator™, Toshiba) based on a conventional infrared location-identification device (Polaris™, Northern Digital) by the install of a volume rendering graphic board (Volume Pro™, Asahi Electronics). The 3-D image was displayed besides the three orthogonal planes display on the computer monitor and the frame rate of the 3-D image was 30 frame/s. The 3D navigation was used in two patients presented with gliomas adjacent to the eloquent brain.

3. Results and conclusion

The frame rate (30 frame/s) could demonstrate the position of the tip of the surgeon's tool real-timely. The 3-D images were acceptable for the surgeons and enough quality for surgeons to comprehend the physical relationship between the region and the other landmarks. We developed the new 3-D navigation system that had fast frame rate and good image quality. The 3-D navigation system updated with intraoperative MRI was advanced system whose display was very useful for surgeons to comprehend the location of the region intuitively.

* Corresponding author. Tel.: +81-33353-8111; fax: +81-35269-7438.
E-mail address: ymuragaki@nij.twmu.ac.jp (Y. Muragaki).

0531-5131/03
doi:10.1016/S0531-5131(03)00308-X

CT and MRI Features of Recurrent Tumors and Second Primary Neoplasms in Pediatric Patients with Retinoblastoma

Ukihide Tateishi[1]
Tadashi Hasegawa[2]
Kunihisa Miyakawa[1]
Minako Sumi[3]
Noriyuki Moriyama[1]

OBJECTIVE. The aim of our study was to describe the CT and MRI findings of recurrent tumors and second primary (malignant and benign) neoplasms in patients with retinoblastoma and to evaluate imaging features to assist in distinguishing them.

MATERIALS AND METHODS. Records of 445 pathologically confirmed retinoblastomas were retrospectively reviewed. Thirty-four patients with recurrent retinoblastomas and 15 patients with second primary neoplasms who underwent CT and MRI were evaluated by two radiologists with agreement by consensus.

RESULTS. Invasive patterns of recurrent tumors included type A, intraocular tumor ($n = 13$); type B, intraorbital tumor with spread into the optic nerve shown as enlargement and marked enhancement of the optic nerve on contrast-enhanced CT or MRI ($n = 6$); and type C, tumor extending to the lateral aspect of the orbit and invading the brain via the sphenoidal bone ($n = 2$). Thirty-eight percent of patients with recurrent tumors had distant metastases ($n = 7$) or leptomeningeal metastases ($n = 6$). Leptomeningeal metastases were found only in recurrent tumors. Second primary neoplasms included osteosarcoma ($n = 5$), rhabdomyosarcoma ($n = 5$), meningioma ($n = 4$), and other tumors ($n = 3$). A significant difference was seen between the patients' ages at the time of diagnosis of recurrent tumors and second primary neoplasms ($p < 0.0001$). Extraorbital tumors were found more frequently among second primary neoplasms than among recurrent tumors ($p < 0.001$).

CONCLUSION. Both recurrent tumors and second primary neoplasms in patients with retinoblastoma often show characteristic imaging features. The tumor distribution on CT and MRI may help in differentiating recurrent tumors and second primary neoplasms.

Retinoblastoma is the most common primary ocular malignancy of early childhood. The tumor is hereditary in all patients with bilateral retinoblastoma and in 10–15% of those with unilateral disease identified by a family history of retinoblastoma [1, 2]. Although the cure rate of retinoblastoma is excellent after enucleation or irradiation, survivors of hereditary retinoblastoma are at increased risk of developing recurrent tumors or second primary (malignant and benign) neoplasms, most commonly osteosarcoma and other soft-tissue sarcomas [1–10]. Loss or mutation of the retinoblastoma gene, which is a prototypical tumor-suppressor gene located on human chromosome 13q14, has been associated with development of other malignancies, including osteosarcoma and other mesenchymal tumors [11–13].

The incidence of second primary neoplasms after retinoblastoma increases with the length of time from initial diagnosis, with a cumulative incidence of 8.4% 18 years after diagnosis [10]. However, a short latency has been found among patients with recurrent tumors, and the incidence may be overestimated because of difficulties in distinguishing second primary neoplasms from recurrent tumors. Second primary neoplasms often show both high-grade and undifferentiated features on microscopic observation, making them difficult to diagnose and distinguish from the small, undifferentiated round cell tumors that are characteristic of recurrent retinoblastomas [14–21]. Although the CT and MRI findings of patients with retinoblastoma are established, there have been only a few descriptions of second primary neoplasms in patients with retinoblastoma [22]. In our study, we retrospectively reviewed and described CT and MRI findings in recurrent tumors and second primary neoplasms in patients with retinoblastoma.

Materials and Methods

We reviewed cross-referenced records from January 1980 to September 2002 in the divisions of radiation oncology and pathology at the National Cancer

Received January 24, 2003; accepted after revision March 27, 2003.

[1]Division of Diagnostic Radiology, National Cancer Center Hospital and Research Institute, 5-1-1, Tsukiji, Chuo-Ku, 104-0045 Tokyo, Japan. Address correspondence to U. Tateishi.

[2]Division of Pathology, National Cancer Center Hospital and Research Institute, Chuo-Ku, 104-0045 Tokyo, Japan.

[3]Division of Radiation Oncology, National Cancer Center Hospital and Research Institute, Chuo-Ku, 104-0045 Tokyo, Japan.

AJR 2003;181:879–884

0361–803X/03/1813–879

Center Hospital, Tokyo, and identified 445 patients with pathologically confirmed retinoblastoma. Of these, 34 patients with recurrent retinoblastomas and 15 patients with second primary neoplasms were included in our study. Of the 15 patients with second primary neoplasms, two patients developed two separate second primary tumors. One child had a temporal rhabdomyosarcoma and developed osteosarcoma 12 years later. Another child first developed meibomian carcinoma in the eyelid, followed 5 years later by a meningioma arising in the skull base. Therefore, we reviewed 15 patients with 17 second primary neoplasms for data analysis. Patients seen in consultation were included in the analysis even if they did not receive all primary therapy for retinoblastoma at our institute because some children were referred with recurrent disease after having initial treatment at an outside institution.

Of the 49 patients evaluated, data regarding age at diagnosis; sex; family history; histologic subtype; location; latent period; and all initial treatment for primary tumors including enucleation, chemotherapy, radiation therapy, and treatment of recurrent tumors and second primary neoplasms were documented. Patients with recurrent tumors or second primary neoplasms received combined modality therapy consisting of surgical resection or biopsy, followed by combination chemotherapy either in standard doses or in escalating doses with autologous bone marrow or peripheral blood stem cell transplantation, with or without radiation therapy. The latent period was calculated from the time of initial diagnosis to the time of diagnosis of recurrent tumors or second primary neoplasms. All tumors in the field of radiation were so classified if they appeared to be originating in the eyelids, orbits, paranasal sinuses, temporal bones, or soft tissues overlying the temporal bone region.

CT and MRI examinations were reviewed by two radiologists with agreement by consensus. The images of 49 patients included both CT and MRI (n = 27), only CT (n = 3), or only MRI (n = 19). Unenhanced CT scans were obtained in 30 patients, and contrast-enhanced CT scans were obtained in 24 patients with the use of IV iodinated contrast material. Section thickness ranged between 5 and 10 mm. CT scans were evaluated for predominant attenuation; homogeneity or heterogeneity; and the presence of calcification, bone destruction, surrounding edema, and tumor enhancement.

MRI was performed using 1.5-T systems. Using the spin-echo technique, we obtained T1-weighted images (TR range/TE range, 400–660/12–15) in the axial and coronal planes. T2-weighted spin-echo or fast spin-echo images (3000–5700/80–118) were then obtained in the axial and coronal planes. Whole-brain images were obtained with a field of view of 30–40 cm, an image matrix of 128 × 256, and a slice thickness of 5–10 mm. Locations were judged by the type of margin, extent of tissue involvement, internal architecture, presence of invasion to surrounding tissue, size, and signal characteristics on T1- and T2-weighted images. Tumor size was determined by the largest diameter in the axial plane of CT scans or MRIs. Locations were correlated with the radiation field in all patients. Signal characteristics were described as hypointense, isointense, or hyperintense relative to the surrounding structures: muscle or white matter. MRIs obtained after the IV administration of a gadolinium chelate with T1-weighting (n = 30) were evaluated for the degree and type of enhancement.

For evaluation of recurrent tumors in patients with retinoblastoma, we categorized growth patterns into three types for assessing recurrent retinoblastoma: intraocular tumor (type A), intraorbital tumor with local spread into the optic nerve (type B), and tumor extending to the lateral aspect of the orbit and invading the brain via the sphenoidal bone (type C).

CT and MRI findings were assessed in both recurrent tumors and each histologic type of second primary neoplasms. We also assessed CT and MRI findings to assist in the differentiation of recurrent tumors and second primary neoplasms.

The data obtained related to disease status regarding retinoblastoma and the second primary neoplasms in all patients. Current status was documented by follow-up examination, and follow-up was calculated in months from the date of initial diagnosis to the most recent follow-up. Differences between subgroups were analyzed for correlations with the chi-square test, Fisher's exact probability test, or Spearman's rank correlation coefficient test. The interobserver variation of the extent of various abnormalities was evaluated with the Spearman's rank correlation coefficient test. A p value of less than 0.05 was considered a statistically significant difference.

Results

Clinical Findings

The clinical features of the patients are summarized in Table 1. A significant difference was seen in age at the time of diagnosis between patients with recurrent tumors and those with second primary neoplasms ($p < 0.0001$). Patients with hereditary tumors developed second primary neoplasms more frequently than they developed recurrent tumors ($p < 0.001$). The initial therapy for patients with both tumor types included combination therapy. No significant difference was found in the radiation dose between recurrent tumors and second primary neoplasms.

The latent period of second primary tumor ranged between 15 and 400 months (median SD, 178.7 ± 28.7 months). There was a signif cant difference in the latent period between re current tumors and second primary neoplasm ($p < 0.0001$). The significant difference was als found in the latent period between histologi subtypes including osteosarcoma, rhabdomyo sarcoma, and meningioma (Table 2). Seventy one percent of patients with recurrent tumor and 73% of patients with second primary neoplasms were still alive, with a median follow-up of 58.2 and 271.3 months, respectively.

Imaging Features in Recurrent Tumors

Sixty-two percent of patients with recurrent tumors had local lesions. Invasive patterns (Fig. 1) of recurrent tumors identified on CT or MRI included type A, intraocular tumor (n = 13, 38%) (Fig. 2); type B, intraorbital tumor with spread into the optic nerve shown as enlargement and marked enhancement of the optic nerve on contrast-enhanced CT or MRI (n = 6, 18%) (Fig. 3); and type C, tumor extending to the lateral aspect of the orbit and invading the brain via the sphenoidal bone (n = 2, 6%) (Fig. 4). Peripherally located intralesional calcification was found in type A (n = 13, 100%) and type B (n = 2, 33%) tumors on unenhanced CT. In addition, no calcification was found in type C tumors. Tumors appeared hypo- to isointense in relation to normal temporal muscle on T1-weighted images and of moderately high signal intensity on T2-weighted images in all patients who underwent MRI. All localized lesions were depicted as heterogeneously enhanced masses with a slightly irregular surface on contrast-enhanced CT or MRI.

Thirty-eight percent of patients with recurrent tumors had distant metastases (n = 7) or leptomeningeal metastases (n = 6) (Fig. 5). Multiple brain metastases were found in three patients. Although the signal characteristics on T1- and

TABLE 1 Characteristics of Patients with Retinoblastoma

Characteristic	Recurrent Tumor	Second Primary Neoplasm	p
No. of patients	34	15	
Age (yr)	2.5 ± 0.4 (0–12)	14.9 ± 2.4 (1–33)	< 0.0001
Sex			NS
Male	21 (62)	7 (47)	
Female	13 (38)	8 (53)	
Family history	7 (21)	1 (7)	NS
Hereditary tumor	6 (18)	12 (80)	< 0.001
Radiation dose (Gy)	40.3 ± 2.1	43.5 ± 2.3	NS
Latent period (mo)	28.5 ± 3.5 (5–79)	178.7 ± 28.7 (15–400)	< 0.0001
Mortality rate	10 (29)	4 (27)	NS

Note.—Numbers in parentheses are percentages or ranges. NS = not significant.

TABLE 2 Second Primary Neoplasms in Patients with Retinoblastoma

Diagnosis	No. of Patients	Size (mm)	Latent Period [a] (mo)
Osteosarcoma	5	50.0 ± 5.4 (45–70)	199.0 ± 54.1 (15–319)
Rhabdomyosarcoma	5	40.0 ± 5.6 (10–80)	55.0 ± 13.8 (15–93)
Meningioma	4	47.5 ± 17.0 (10–80)	291.3 ± 47.3 (169–400)
Malignant fibrous histiocytoma	1	35	192
Meibomian gland carcinoma	1	20	248

Note.—Numbers in parentheses are ranges.

[a] Significant difference was found in latent period among osteosarcoma, rhabdomyosarcoma, and meningioma by Spearman's rank correlation coefficient test ($p < 0.05$).

T2-weighted images were nonspecific, lesions showed heterogeneous enhancement on contrast-enhanced CT or MRI. One patient developed skull metastasis that was seen as focal bone destruction on unenhanced CT and a moderately enhanced mass on contrast-enhanced MRI.

Imaging Features in Second Primary Neoplasms

Seventeen second primary neoplasms included various histologic types of tumors. Malignant tumors consisted of osteosarcoma ($n = 5$), rhabdomyosarcoma ($n = 5$), malignant fibrous histiocytoma ($n = 1$), and meibomian gland carcinoma ($n = 1$), whereas benign tumors were meningioma ($n = 4$) (Table 2).

Osteosarcoma was one of the frequent histologic subtypes (29%). Tumors originated from previously irradiated regions, including the intraorbit ($n = 2$), temporal bone ($n = 1$), and ethmoid bone ($n = 1$). One patient developed a tumor in the distal femur outside the irradiated field. Unenhanced CT scans revealed irregular masses in the orbit, temporal bone, or ethmoid bone with calcification ($n = 4$, 80%) (Fig. 6). Two tumors showed severe bone destruction on unenhanced CT. Contrast-enhanced CT and MRI showed heterogenous enhancement with perifocal edema ($n = 5$, 100%). Fluid–fluid levels, suggestive of hemorrhage, were identified in two tumors on T2-weighted images. Calcification identified on unenhanced CT corresponded in part to areas of signal voids or low signal intensity on both T1- and T2-weighted images.

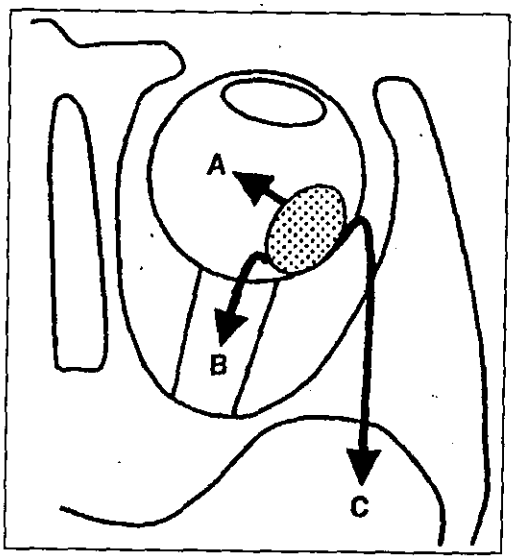

1

Fig. 1.—Drawing shows types of tumor extension in recurrent retinoblastoma. Three growth patterns are present in recurrent retinoblastoma: intraocular tumor (type A), intraorbital tumor with local spread into optic nerve (type B), and tumor extending to lateral aspect of orbit and invading brain via sphenoidal bone (type C).

2

Fig. 2.—2-year-old boy with recurrent retinoblastoma who underwent enucleation of left eye and irradiation of both eyes. Axial T2-weighted image (TR/TE, 4000/118) shows soft-tissue mass in right globe (type A). Tumor (*arrowheads*) shows heterogeneous high signal intensity relative to temporal muscle.

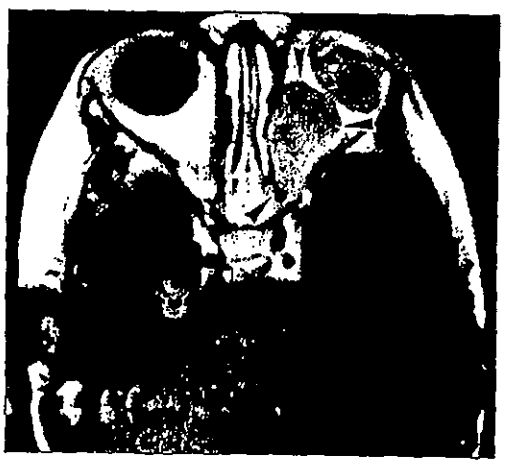

3

Fig. 3.—3-year-old boy with recurrent retinoblastoma who underwent irradiation of left eye. Axial contrast-enhanced T1-weighted image (TR/TE, 630/15) shows recurrent tumor (*arrowheads*) that extended into optic nerve (type B) with heterogeneous enhancement.

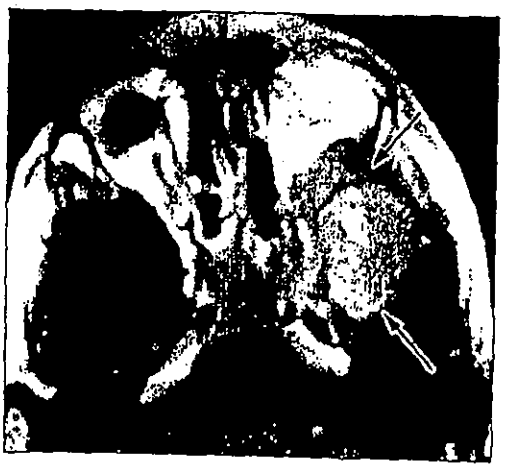

4

Fig. 4.—6-year-old boy with recurrent retinoblastoma who underwent enucleation and irradiation of left eye. Axial contrast-enhanced T1-weighted image (TR/TE, 600/15) shows tumor extension (*arrows*) through greater wing of sphenoid to middle cranial fossa (type C).

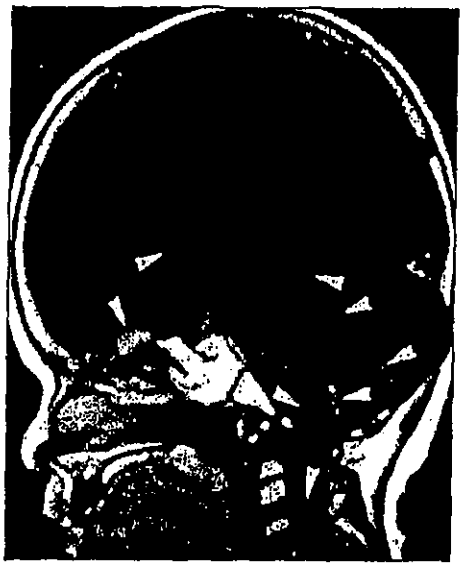

Fig. 5.—4-year-old boy with recurrent retinoblastoma who underwent enucleation, irradiation, and chemotherapy. Coronal contrast-enhanced T1-weighted image (TR/TE, 400/15) shows multiple leptomeningeal metastases (*arrowheads*).

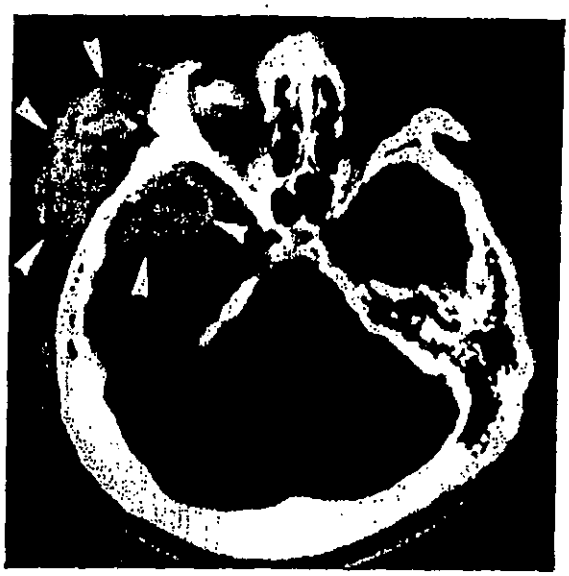

Fig. 6.—Osteosarcoma in 25-year-old man with hereditary retinoblastoma who underwent enucleation, irradiation, and chemotherapy of both eyes. Axial CT scan shows faintly calcified mass (*arrowheads*) of temporal bone invading both brain and soft tissues.

All rhabdomyosarcomas arose in the region previously irradiated, including five tumors that developed in the temporal muscle within the irradiated field and one that involved the contralateral temporal muscle, which may have received a radiation dose of 50–60% of that in the irradiated field. Unenhanced CT revealed well-defined masses with ovoid contours situated in the temporal muscle ($n = 5$, 100%). Five patients underwent both contrast-enhanced CT and MRI; of these, three tumors (60%) showed heterogeneous and slight enhancement relative to the adjacent muscle (Fig. 7). Fluid–fluid levels were found in one tumor on both T1- and T2-weighted images. Signal characteristics on T1- and T2-weighted images were nonspecific in the other four tumors.

A 16-year-old girl with hereditary retinoblastoma developed malignant fibrous histiocytoma in the orbit, with severe destruction of bone identified on unenhanced CT (Fig. 8). The tumor showed nonspecific signal characteristics on T1- and T2-weighted images, but marked enhancement was found on contrast-enhanced CT scans and MRIs. A 20-year-old woman developed a well-defined mass in the eyelid that was seen on unenhanced CT and diagnosed as a meibomian gland carcinoma after a latent period of 121 months. The tumor showed nonspecific signal characteristics on both T1- and T2-weighted images, but areas of marked enhancement were found on contrast-enhanced MRIs (Fig. 9).

All meningiomas originated from the previously irradiated skull base. Tumors showed hyperattenuation on unenhanced CT ($n = 4$), and marked enhancement was found in all cases on contrast-enhanced CT and MRI (Fig. 10). Punctate calcification was found in one case; this tumor was associated with secondary hyperplastic change of the adjacent bone. Signal characteristics were nonspecific on T1- and T2-weighted images. However, perifocal edema was found in three cases in the adjacent white matter on T2-weighted images.

Differentiation Between Recurrent Tumors and Second Primary Neoplasms

Peripherally located intralesional calcification was found in all type A and in 33% of type B tumors on unenhanced CT. However, this finding was similar to that of osteosarcoma arising in the orbit. Three invasive patterns of recurrent tumors were identified on CT or MRI, whereas only two patients with second primary tumors showed these patterns. However, this configuration of invasive patterns did not assist in the differentiation of recurrent tumors and second primary neoplasms (Table 3). Brain metastases and leptomeningeal metastases were found only in recurrent tumors. A statistically significant difference was found in intra- and extraorbital location of tumors between recurrent tumors and second primary neoplasms (Table 4).

Discussion

In our study, we described the CT and MRI findings of both recurrent tumors and second

Fig. 7.—Rhabdomyosarcoma in 5-year-old girl with retinoblastoma who underwent irradiation in right eye. Axial T2-weighted image (TR/TE, 5700/105) shows well-defined soft-tissue mass arising from deep aspect of temporal muscle. Tumor (*arrowheads*) shows high signal intensity relative to muscle.

Fig. 8.—Malignant fibrous histiocytoma in 16-year-old girl with hereditary retinoblastoma who underwent enucleation and irradiation in right eye. Axial contrast-enhanced CT scan shows irregular mass (*arrow*) with bone destruction in orbit.

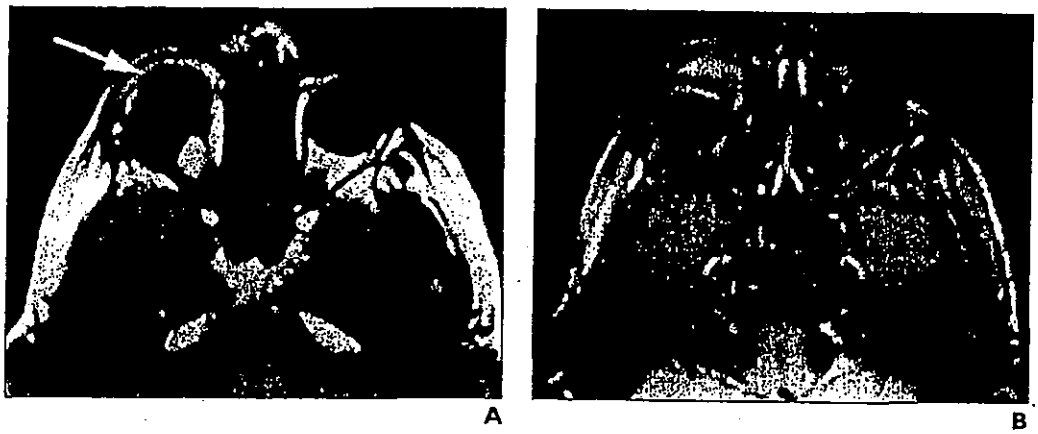

Fig. 9.—Meibomian gland carcinoma in 20-year-old woman with hereditary retinoblastoma who underwent enucleation and irradiation.
A, Axial T1-weighted image (TR/TE, 600/15) shows well-defined soft-tissue mass (*arrow*) in orbit.
B, Axial contrast-enhanced T1-weighted image (600/15) shows marked enhancement of tumor.

primary neoplasms in patients with retinoblastoma. The short latency among patients with retinoblastoma is one factor that encourages us to question whether their new lesions are recurrent tumors or second primary neoplasms. Second primary neoplasms tend to appear after longer intervals, usually showing a latent period of at least 10 years [1, 2]. This finding was mostly in accordance with our results. However, two cases of second primary neoplasms had much shorter latent periods of 15 months. Our results show that both the recurrent tumors and the second primary neoplasms may be seen in the same latent periods. The type of second primary neoplasm appears to be related to the latent period. Rhabdomyosarcoma seems to occur earlier than other tumors, with a relatively short latency ranging from 15 to 93 months. Osteosarcoma is usually considered to be the most frequent second primary tumor in patients with hereditary retinoblastoma. The relatively short follow-up periods in earlier studies probably gave the misleading impression that it is osteosarcoma that preferentially develops in patients who have survived a hereditary tumor at an earlier age than other types of second primary neoplasms.

CT and MRI can show tumor extension by three types of growth patterns in primary retinoblastoma: the endophytic type, in which the tumor projects anteriorly and grows into the vitreous; the exophytic type, in which the tumor arises intraretinally and subsequently grows into the subretinal space; and the diffuse infiltrating type, in which tumor growth in the retina appears as a plaquelike mass [14–16]. Our results also suggested that three growth patterns might exist in recurrent retinoblastoma, and that CT and MRI can detect tumor extension: intraocular tumor (type A), intraorbital tumor with local spread into the optic nerve (type B), and tumor extending to the lateral aspect of the orbit and invading the brain via the sphenoidal bone (type C).

Different types of second primary neoplasms have also been documented in previous studies, with most of the second primary neoplasms being soft-tissue sarcomas, followed by melanomas, brain tumors, leukemias, and other epithelial tumors [1–9]. In our study, the most common types of second primary neoplasms in patients with retinoblastoma were osteosarcoma and rhabdomyosarcoma.

Osteosarcoma is one of the most frequent second primary neoplasms originating from a previously irradiated region. Calcification within the tumor that depends on the amount of mineralization is observed on CT. Four of our patients showed central calcification within the mass on unenhanced CT. An important feature to diagnose osteosarcoma on CT may be central calcification within the mass situated in the irradiated field, including the intraorbit, temporal bone, and ethmoid bone. Extraskeletal osteosarcoma presents nonspecific signal characteristics on MRI: a mass with mixed low signal intensity on T1-weighted images and mixed but predominantly high signal intensity on T2-weighted images [23–25]. Fluid–fluid levels, suggestive of hemorrhage, were identified in two of our patients on T2-weighted images; this finding was consistent with a previous report [23].

Rhabdomyosarcoma also presents with rather nonspecific CT and MRI findings, but some characteristic findings were discovered in our patients. All rhabdomyosarcomas arose within the region previously irradiated. As a rule, rhabdomyosarcomas in the head and neck region grow rapidly, often in an infiltrative and destructive manner [26, 27]. However, all of our patients presented with well-defined masses with ovoid contours situated in the temporal muscle on both CT and MRI. The MRI

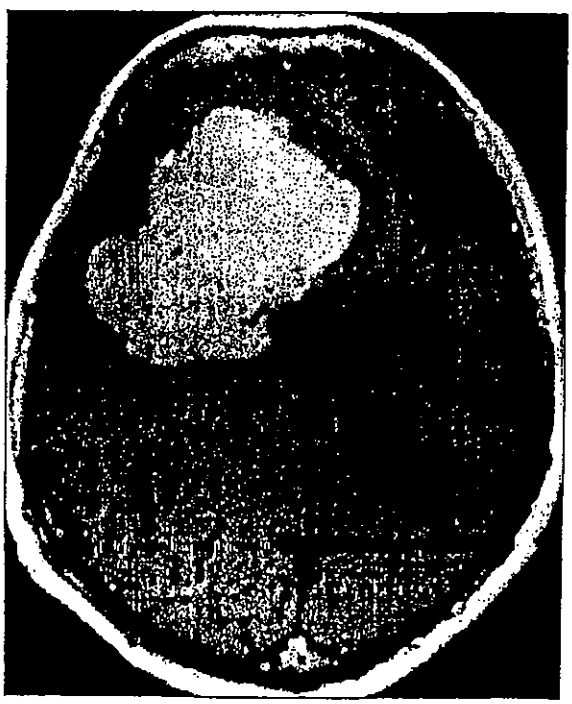

Fig. 10.—Meningioma in 24-year-old man with hereditary retinoblastoma who underwent enucleation and irradiation. Axial contrast-enhanced T1-weighted image (TR/TE, 600/15) shows extraaxial mass with marked enhancement adjacent to sphenoid bone.

TABLE 3 Invasive Patterns in Recurrent Tumors and Second Primary Neoplasms

Invasive Types	Type A		Type B		Type C	
	No.	%	No.	%	No.	%
Recurrent tumor (n = 21)	13	62	6	29	2	9
Second primary neoplasm (n = 2)	0		1	50	1	50

Note.—Patients with distant metastases are excluded. Invasive patterns do not help to distinguish recurrent tumors and second primary neoplasms by Spearman's rank correlation test (p = 0.11). Type A = intraocular tumor, type B = intraorbital tumor with spread into optic nerve, type C = tumor extending to lateral aspect of orbit and invading brain via sphenoidal bone.

TABLE 4 Intra- and Extraorbital Tumor Location

Characteristics	Intraorbital		Extraorbital	
	No.	Range	No.	Range
Recurrent tumor (n = 34)	21	62	13	38
Second primary neoplasm (n = 17)	2	11	15	88

Note.—Significant difference was found between two groups by Fisher's exact probability test (p < 0.001).

signal characteristics and enhancement patterns identified on both contrast-enhanced CT and MRI were nonspecific. Few characteristic imaging findings reflect the degree of cellularity; the relative amounts of collagen; and the presence and extent of secondary changes such as hemorrhage, necrosis, and ulceration.

The initial therapy for primary tumors has been enucleation of the most severely affected eye and irradiation of the contralateral eye to preserve vision. Patients with hereditary retinoblastoma may have an increased susceptibility to the induction of second primary neoplasms by radiation [28].

Radiation increases the total risk in addition to the already high incidence because more second primary tumors develop in the irradiated field than outside the irradiated field [2]. Sarcomas can be categorized as radiation-induced if they meet the following criteria: tumor must develop within the boundaries of a previously irradiated area, a relatively long asymptomatic latent period (≥ 4 years) must have elapsed, the tumor must have a different histology from the original lesion, and the tumor must be histologically confirmed [28]. Most of our cases of second primary neoplasms arose in the irradiated field. However, some tumors occurred with relatively short latency and outside the irradiation field. Similar findings have suggested that nearly all second primary neoplasms occur among hereditary retinoblastoma tumors, and that many second primary tumors occur outside the irradiation field, with some among nonirradiated tumors [2, 28]. Second primary neoplasms in patients with retinoblastoma may occur both as a result of, and independently of, radiation therapy. However, the follow-up period and the number of patients with second primary neoplasms in our study are not sufficient for conclusive analysis. Further follow-up study is necessary to evaluate the relationship between irradiation and the occurrence of second primary neoplasms in patients with retinoblastoma.

In conclusion, several kinds of imaging features were present both in recurrent tumors and in second primary neoplasms in patients with retinoblastoma. The tumor distribution on CT and MRI may help in differentiating recurrent tumors and second primary neoplasms.

References

1. Smith LM, Donaldson SS, Egbert PR, Link MP, Bagshaw MA. Aggressive management of secondary primary tumors in survivors of hereditary retinoblastoma. *Int J Radiat Oncol Biol Phys* 1989;17:499–505
2. Abramson DH, Ellsworth RM, Kitchin FD, Tung G. Second nonocular tumors in retinoblastoma survivors: are they radiation-induced? *Ophthalmology* 1984;91:1351–1355
3. Derkinderen DJ, Kolen JW, Nagelkerke NJD, Tan KE, Beemer FA, Den Otter W. Non-ocular cancer in patients with hereditary retinoblastoma and their relatives. *Int J Cancer* 1988;41:499–504
4. Dickman PS, Barmada M, Gollin SM, Blatt J. Malignancy after retinoblastoma: secondary cancer or recurrence? *Hum Pathol* 1997;28:200–205
5. Draper GJ, Sanders BM, Kingston JE. Second primary neoplasms in patients with retinoblastoma. *Br J Cancer* 1986;53:661–671
6. Dunkel IJ, Gerald WL, Rosenfield NS, Strong EW, Abramson DH, Ghavimi F. Outcome of patients with a history of bilateral retinoblastoma treated for second malignancy: the Memorial Sloan-Kettering experience. *Med Pediatr Oncol* 1998;30:59–62
7. Chemello PD, Nelson CL, Tomich CE, Sadove AM. Embryonal rhabdomyosarcoma arising in the masseter muscle as a second malignant neoplasm. *J Oral Maxillofac Surg* 1988;46:899–905
8. Hasegawa T, Matsuno Y, Niki T, et al. Second primary rhabdomyosarcomas in patients with bilateral retinoblastoma: a clinicopathologic and immunohistochemical study. *Am J Surg Pathol* 1998;22:1351–1360
9. Walford N, Deferrai R, Slater RM, et al. Intraorbital rhabdoid tumour following bilateral retinoblastoma. *Histopathology* 1992;20:170–173
10. Moll AC, Imhof SM, Bouter LM, Tan KE. Second primary tumors in patients with retinoblastoma: a review of the literature. *Ophthalmic Genet* 1997;18:27–34
11. Scholz RB, Kabisch H, Delling G, Winkler K. Homozygous deletion within the retinoblastoma gene in a native osteosarcoma specimen of a patient cured of a retinoblastoma of both eyes. *Pediatr Hematol Oncol* 1990;7:265–273
12. Issing WJ, Wustrow TP, Oeckler R, Mezger J, Nerlich A. An association of the RB gene with osteosarcoma: molecular genetic evaluation of a case of hereditary retinoblastoma. *Eur Arch Otorhinolaryngol* 1993;250:277–280
13. Rieder H, Lohmann D, Poensgen B, et al. Loss of heterozygosity of the retinoblastoma (*RB1*) gene in lipomas from a retinoblastoma patient. *J Natl Cancer Inst* 1998;90:324–326
14. Mafee MF, Goldberg MF, Greenwald MJ, Schulman J, Malmed A, Flanders AE. Retinoblastoma and simulating lesions: role of CT and MR imaging. *Radiol Clin North Am* 1987;25:667–682
15. Danziger A, Prince HI. CT findings in retinoblastoma. *AJR* 1979;133:695–697
16. Kaufman LM, Mafee MF, Song CD. Retinoblastoma and simulating lesions: role of CT, MR imaging, and use of Gd-DTPA contrast enhancement. *Radiol Clin North Am* 1998;36:1101–1117
17. Brisse HJ, Lumbroso L, Freneaux PC, et al. Sonographic, CT, and MR imaging findings in diffuse infiltrative retinoblastoma: report of two cases with histologic comparison. *AJNR* 2001;22:499–504
18. Beets-Tan RG, Hendriks MJ, Ramos LM, Tan KE. Retinoblastoma: CT and MRI. *Neuroradiology* 1994;36:59–62
19. O'Brien JM. Retinoblastoma: clinical presentation and the role of neuroimaging. *AJNR* 2001;22:426–428
20. Char DH, Hedges TR, Norman D. Retinoblastoma: CT diagnosis. *Ophthalmology* 1984;91:1347–1350
21. Arrigg PG, Hedges TR, Char DH. Computed tomography in the diagnosis of retinoblastoma. *Br J Ophthalmol* 1983;67:588–591
22. Chan LL, Czerniak BA, Ginsberg LE. Radiation-induced osteosarcoma after bilateral childhood retinoblastoma. *AJR* 2000;174:1288
23. Murphey MD, Robbin MR, McRae GA, Flemming DJ, Temple HT, Kransdorf MJ. The many faces of osteosarcoma. *RadioGraphics* 1997;17:1205–1231
24. Moser RP Jr. Musculoskeletal case of the day: extraskeletal osteosarcoma of the thigh. *AJR* 1994; 162:1463–1465
25. Varma DG, Ayala AG, Guo SQ, Moulopoulos LA, Kim EE, Chamsangavej C. MRI of extraskeletal osteosarcoma. *J Comput Assist Tomogr* 1993;17:414–417
26. Lee JH, Lee MS, Lee BH, et al. Rhabdomyosarcoma of the head and neck in adults: MR and CT findings. *AJNR* 1996;17:1923–1928
27. Yang WT, Kwan WH, Li CK, Metreweli C. Imaging of pediatric head and neck rhabdomyosarcomas with emphasis on magnetic resonance imaging and a review of the literature. *Pediatr Hematol Oncol* 1997;14:243–257
28. Schwarz MB, Burgess LP, Fee WE, Donaldson SS. Postirradiation sarcoma in retinoblastoma: induction or predisposition? *Arch Otolaryngol Head Neck Surg* 1988;114:640–644